

Title: Circulating immunome fingerprint in eosinophilic esophagitis is associated with clinical response to proton pump inhibitor treatment

Authors:

Lola Ugalde-Triviño^{1,2*}, Francisca Molina-Jiménez^{1,2*}, Juan H-Vázquez^{3*}, Carlos Relaño-Rupérez^{1,2,4}, Laura Arias-González^{2,6,7,8}, Sergio Casabona^{2,9}, María Teresa Pérez-Fernández^{2,9}, Verónica Martín-Domínguez^{2,9}, Jennifer Fernández-Pacheco^{2,9}, Alfredo J Lucendo^{2,6,7,8}, David Bernardo^{3,5,&#}, Cecilio Santander^{2,8,9,&#}, Pedro Majano^{1,2,8,10,&#}

1. Molecular Biology Unit, Hospital Universitario de la Princesa, Madrid, Spain.
2. Instituto de Investigación Sanitaria Hospital Universitario de La Princesa (IIS-Princesa), Madrid, Spain.
3. Mucosal Immunology Lab, Centro de Investigaciones Biomédicas en Red de Enfermedades Infecciosas (CIBERINFEC), Unidad de Excelencia Instituto de Biología y Genética Molecular (IBGM), Universidad de Valladolid, 47005 Valladolid, Spain.
4. Bioinformatics Unit, Centro Nacional de Investigaciones Cardiovasculares (CNIC), Madrid, Spain
5. Centro de Investigación Biomédica en Red de Enfermedades Infecciosas (CIBERINFEC), 28029 Madrid, Spain
6. Department of Gastroenterology, Hospital General de Tomelloso, Tomelloso, Ciudad Real, Spain.
7. Instituto de Investigación Sanitaria de Castilla-La Mancha (IDISCAM), Spain.
8. Centro de Investigación Biomédica en Red de Enfermedades Hepáticas y Digestivas (CIBERehd), Madrid, Spain.
9. Department of Gastroenterology, Hospital Universitario de La Princesa, Madrid, Spain.
10. Department of Cellular Biology, Faculty of Biology, Universidad Complutense de Madrid, Madrid, Spain.

* Co-first author

& Senior author

#Correspondence to:

Pedro L Majano, PhD
Hospital Universitario de la Princesa
Instituto Investigación Sanitaria Princesa (IP)
Diego de León 62
28006. MADRID. Spain
(pmajano@ucm.es / pedro.majano@salud.madrid.org)

Dr. Cecilio Santander, MD, PhD
Head of Department of Gastroenterology
Hospital Universitario de La Princesa
Instituto de Investigación Sanitaria Princesa IIS-IP
Madrid. Spain
(cecilio.santander@salud.madrid.org)

48
49 David Bernardo, PhD
50 Mucosal Immunology Lab, Universidad de Valladolid
51 Unidad de Excelencia Instituto de Biología y Genética Molecular (IBGM)
52 Centro de Investigaciones Biomédicas en Red de Enfermedades Infecciosas
53 (CIBERINFEC)
54 (d.bernardo.ordiz@gmail.com / david.bernardo@uva.es)
55
56

57 **AUTHOR CONTRIBUTIONS**

58 Conceived and designed the study: AJL, DB, CS, PM.
59 Participated in the clinical management of patients: SC, MTF-P, VM-D, JF-P, CS.
60 Performed the experiments: LU-T, FM-J, JH-V, LA-G, PM.
61 Analysed and discussed the data: LU-T, FM-J, JH-V, CR-R, DB, PM.
62 Wrote the paper: LU-T, DB, JH-V, CS, PM.
63 All the authors read, provided comments, and approved the final version of the
64 manuscript.
65

66 **AUTHOR DISCLOSURE**

67 None to declare
68

69 **ORCID NUMBERS**

70 Lola Ugalde-Triviño: 0000-0002-0911-8043
71 Francisca Molina-Jiménez: 0000-0003-4912-1025
72 Juan H-Vázquez: 0000-0002-4805-2403
73 Carlos Relaño-Rupérez: 0000-0002-1407-9245
74 Laura Arias-González: 0000-0003-2132-9350
75 Sergio Casabona: 0000-0002-6131-8341
76 María Teresa Pérez-Fernández: 0000-0003-0363-2516
77 Verónica Martín-Domínguez: 0000-0001-6839-2707
78 Jennifer Fernández-Pacheco 0000-0002-5384-0658
79 Alfredo J Lucendo: 0000-0003-1183-1072
80 David Bernardo: 0000-0002-2843-6696
81 Cecilio Santander: 0000-0001-5492-2535
82 Pedro Majano: 0000-0002-5495-1413
83

84

85

86

87

88

89

90

91 WHAT IS KNOWN

- 92 • Eosinophilic esophagitis (EoE) is a Th2 type immune disorder with increased
- 93 prevalence in the last years.
- 94 • Proton pump inhibitor (PPI) treatment is the preferred first-line therapy for
- 95 EoE, which leads to clinical and pathological reversion in about half of the
- 96 cases. Non-responding patients require other therapeutic options.
- 97 • Currently, an endoscopy with esophageal biopsies is required for EoE
- 98 diagnosis and to monitor response to treatment. Therefore, the discovery of
- 99 non-invasive biomarkers is of utmost importance for treatment monitoring.
- 100 • To date only peripheral eosinophil and Th2 profiles have been studied in EoE.

102 WHAT IS NEW HERE

- 103 • At diagnosis EoE patients have a specific circulating immune signature.
- 104 • PPI-responding and non-responding EoE patients have different immune
- 105 fingerprints at baseline.
- 106 • Immune characterization of EoE patients at diagnosis and after PPI treatment
- 107 unveiled differential levels of circulating plasmacytoid dendritic cells (pDCs)
- 108 depending on their inflammatory state and response to PPI treatment. Those
- 109 levels are related with the number of pDCs infiltrated in the esophageal tissue.

111

112

113

114

115

116

117

118

119

120

121

122

123

124

125

126

127 ABSTRACT

128 **Objectives:** The aim of the study was to characterize the circulating immunome of
129 patients with EoE before and after proton pump inhibitor (PPI) treatment in order to
130 identify potential non-invasive biomarkers of treatment response.

131 **Methods:** PBMCs from 19 healthy controls and 24 EoE patients were studied using a
132 39-plex spectral cytometry panel. The plasmacytoid dendritic cell (pDC) population was
133 differentially characterized by spectral cytometry analysis of immunofluorescence
134 assays in esophageal biopsies from 7 healthy controls and 13 EoE patients.

135 **Results:** Interestingly, EoE patients at baseline had lower levels of circulating pDC
136 compared with controls. Before treatment, patients with EoE who responded to PPI
137 therapy had higher levels of circulating pDC and classical monocytes, compared with
138 non-responders. Moreover, following PPI therapy pDC levels were increased in all EoE
139 patients, while normal levels were only restored in PPI-responding patients. Finally,
140 circulating pDC levels inversely correlated with peak eosinophil count and pDC count in
141 esophageal biopsies. The number of tissue pDCs significantly increased during active
142 EoE, being even higher in non-responder patients when compared to responder
143 patients pre-PPI. pDC levels decreased after PPI intake, being further restored almost
144 to control levels in responder patients post-PPI.

145 **Conclusions:** We hereby describe a unique immune fingerprint of EoE patients at
146 diagnosis. Moreover, circulating pDC may be also used as a novel non-invasive
147 biomarker to predict subsequent response to PPI treatment.

148

149 KEY WORDS

150 Spectral cytometry, Biomarker, Eosinophilic esophagitis, Plasmacytoid dendritic cells

151

152 ABBREVIATIONS

153

154 EoE: Eosinophilic esophagitis
155 EoEHSS: Eosinophilic Esophagitis Histologic Scoring System
156 EREFS: EoE endoscopic reference score
157 GERD: Gastro-esophageal reflux disease.
158 LN: Lymph node
159 LogFC: Log2 Fold Change
160 NR: Non-responder
161 PBMCs: Peripheral blood mononuclear cells
162 pDC: Plasmacytoid dendritic cells
163 PPI: Proton Pump Inhibitors
164 R: Responder
165 Th2: T helper 2 cells
166 UMAP: Uniform Manifold Approximation and Projection

167

168

169

170

171

172 **FINANCIAL SUPPORT**

173 PM and CS are supported by grants PI17/0008 and ISCIII-Proteored 2019 of Instituto
 174 de Salud Carlos III (ISCIII, Spain) and co-funded by Fondo Europeo de Desarrollo
 175 Regional (FEDER). CS is also funded by Asociación Española de Gastroenterología
 176 (AEG) 2019 grant. DB is funded through the Spanish Ministry of Science [PID2019-
 177 104218RB-I00], Programa Estratégico Instituto de Biología y Genética Molecular
 178 (IBGM Junta de Castilla y León. Ref. CCVC8485) and the European Commission –
 179 NextGenerationEU (Regulation EU 2020/2094), through CSIC's Global Health
 180 Platform. LU-T is recipient of an INVESTIGO contract from Comunidad de Madrid (09-
 181 PIN1-00015.6/2022) partly funded by the European Social Fund, NextGenerationEU,
 182 and Recovery, Transformation and Resilience Plan. CR-R is recipient of an
 183 INVESTIGO contract from Ministry of Labour and Social Economy, the national public
 184 employment service (SEPE) (INVESTIGO Exp. 2022-C23.I01.P03. S0020-0000031)
 185 partly funded by the European Social Fund, NextGenerationEU, and Recovery,
 186 Transformation and Resilience Plan.

187

188 **ACKNOWLEDGMENTS**

189 We acknowledge, Instituto de Salud Carlos III, FEDER organization, Spanish
 190 Gastroenterology Association and Spanish Ministry of Science for the support to this
 191 study. Also, we would like to acknowledge the support from European Social Fund,
 192 NextGenerationEU, and Recovery, Transformation and Resilience Plan. We express
 193 our gratitude to Dr. Manuel Gómez for critical review of the manuscript and English
 194 editing.

195

196

197

198 **Word count:** 3856

199

200

201

202

203

204

205

206

207

208

209

210

211

212

213

214

215

216

217

218

219

220

221

222 INTRODUCTION

223

224 Eosinophilic esophagitis (EoE) is a Th2-type immune disorder which is considered an
225 increasing leading cause of chronic esophageal dysfunction in patients of all ages^{1,2}
226 just after gastro-esophageal reflux disease (GERD).

227 Eosinophils are normally found in the gastrointestinal tract; however, they are absent
228 from the esophageal tissue in health conditions. In EoE, the eosinophil infiltrate in the
229 esophageal tissue layers^{3,4} leads to tissue remodelling and fibrosis as well as
230 subsequent dysfunction characterized by esophageal dysmotility, narrowing and
231 rigidity⁵. As a result, patients experience food impaction, dysphagia and heartburn
232 among other symptoms, which impair their health-related quality of life. Therefore, an
233 early EoE diagnosis and effective therapy are essential to prevent impairment of
234 esophageal function. EoE patients often have concurrent allergic responses to food
235 and airborne allergens, together with a yet unexplained male predominance^{6,7}.

236 First-line therapeutic options for EoE include dietary restrictions, protein pump inhibitor
237 (PPI) therapy and swallowed topical corticosteroids, which provide variable
238 effectiveness⁸⁻¹². Recently, the anti-interleukin-4 receptor antagonist dupilumab joined
239 the therapeutic armamentarium against EoE^{13,14}. Among them, PPI represent the
240 preferred therapy in clinical practice, despite its limited effectiveness¹⁵; histologic
241 remission and clinical improvement after PPI are achieved by only 50% and 70% of
242 treated patients, respectively¹⁶. Patients who do not respond to PPI require
243 subsequent therapeutic options.

244 Currently, EoE diagnosis and treatment response monitoring require endoscopy with
245 esophageal biopsies, as clinical symptoms do not correlate well with esophageal
246 inflammation^{17,18}. In this regard, the chronic nature of this disease together with the
247 dissociation between patients' symptoms and esophageal inflammation¹⁸ require
248 seeking for novel reliable biomarkers and clinical parameters able to identify patient
249 profiles at diagnosis and follow-up. Recent studies have focused on seeking for new
250 biomarkers by characterizing the RNA¹⁹⁻²¹ and proteomic profile of EoE at esophageal
251 tissue level²². Nevertheless, these approaches are still invasive. Hence, the
252 development of novel non-invasive biomarkers to aid on EoE diagnosis and monitoring
253 is an essential unmet need²³.

254 Building from all these precedents, in this study we aimed to characterize the
255 circulating immunome of EoE patients at the time of diagnosis using top-of-the-art
256 spectral cytometry. With this approach, we expected to identify specific immune
257 subsets that could not only help to characterize this disorder, but also to identify novel
258 non-invasive biomarkers able to predict response to PPI treatment.

259

260

261 MATERIAL AND METHODS

262

263 Human subjects

264

265 A total of 25 incident adult EoE patients were prospectively recruited at the moment of
266 diagnosis at Hospital Universitario de La Princesa (Madrid, Spain) between February
267 2018 and November 2020. EoE was diagnosed according to evidence-based

guidelines³ including: (i) symptoms referring to esophageal dysfunction, (ii) infiltration of the esophageal epithelium by 15 or more eosinophils per high-powered field (hpf) assessed from 6 endoscopic biopsy samples; (ii) absence of eosinophilic infiltration in biopsy specimens from gastric and duodenal mucosa; and (iii) exclusion of alternative potential causes of esophageal eosinophilia. Subjects (n=19) who underwent upper endoscopy for assessment of dyspepsia or suspected gastroduodenal ulcer were included as controls. Esophageal biopsies obtained in the endoscopy were normal in all cases and eosinophilic infiltration was excluded. All controls with hiatus hernia, incompetent cardias, or esophageal peptic lesions were excluded hence ensuring that all the recruited controls displayed a normal endoscopic appearance and eosinophil-free biopsies of the esophagus.

Atopic background was recorded for all EoE patients and control subjects. The EoE endoscopic reference score (EREFS) rating the severity of esophageal inflammation (oedema, furrows, exudates) and fibrosis (rings and stricture)²⁴ was assessed in all patients. Furthermore, the validated Eosinophilic Esophagitis Histologic Scoring System (EoEHSS) was also determined, evaluating eight pathologic features for both severity (grade) and extent (stage) of abnormalities²⁵.

Out of the 25 EoE patients, 18 underwent double dose PPI treatment (omeprazole 20 mg b.i.d. or equivalent) for an 8-week period, after which they were classified as responders (n=9) or non-responders (n=9) based on the peak eosinophil count in a second endoscopy in which EREF and EoEHSS scores were also assessed. The study was approved by the local Ethics Committee (PI17/0008, registry number 3107, 8 June 2017). All individuals provided written informed consent.

Blood samples

In all cases, blood samples were obtained at the time of the endoscopy from EoE patients (both before and after PPI-treatment in the latter) and controls. After placing a venous line to provide sedation for endoscopy, blood was collected in EDTA-coated tubes to isolate peripheral blood mononuclear cells (PBMC).

PBMCs staining and spectral cytometry acquisition

PBMCs were isolated by Ficoll gradient assay. Viable cells were counted and cryopreserved in freezing medium (Foetal bovine serum [Hyclone, Thermofisher] complemented with DMSO 20% medium) at vapour phase of liquid nitrogen.

For the analysis, PBMCs were thawed and a total of 2 million PBMCs were stained with monoclonal antibodies (Supplementary Table 1) applying a modified OMIP-69 panel protocol²⁶. Before staining, Live/Dead fixable blue dead cell stain kit was added to exclude dead cells from the analysis. Brilliant Stain Buffer and True-Stain Monocyte Blocker were also added before staining with the aim of obtaining the optimal fluorescence. PBMCs were washed with FACS buffer (500mL PBS +1 0mL filtered FCS + 0.1g NaN₃ + 2.5mL sterile EDTA) and incubated in the dark at room temperature during staining. Cells were further fixed in 0.8% paraformaldehyde in FACS buffer in the dark for 10min and washed with FACS buffer. Cells were preserved at 4°C until acquired (within 48h) in a 5-laser spectral cytometer (Aurora, Cytex).

Cytometry data and statistical analysis

Spectral cytometry data were analysed using the OMIQ Data Science platform (© Omiq, Inc. 2022). After setting the scale, parameters, and cofactors, the FlowAI

algorithm was used for cleaning the data from aberrant signal patterns or events. Then, cell debris and doublets were excluded to gate viable leukocytes (CD45⁺) where an unsupervised approach was applied with a dimensionality reduction Uniform Manifold Approximation and Projection (UMAP)²⁷ plus clustering FlowSOM algorithms. Merging these two algorithms allows a deeper classification of the different immune subsets through different marker expression on the UMAP. A heatmap was also built showing the expression levels of each marker within each cluster. Dendrograms further grouped the clusters and markers associated by similarity.

Statistical analysis was performed in all cases using Rstudio 2022.07.2+576. Differential analysis of clusters defined in OMIQ was performed with the edgeR package, using genewise quasi-likelihood (QL) F-tests with GLMs. Significance was set at p -values ≤ 0.05 and Log2 Fold Change (LogFC) ≥ 1.5 . Differences between groups of significant clusters were validated by classic gating strategy approaches (Supplementary Figure 1 and 2). Manual gating results were analysed by *t*-test (paired when indicated) and/or two-way ANOVA test followed by *post hoc* Fisher test. Outliers were determined through Grubbs' test and deleted from the final analysis. Statistical significance was considered when p -value ≤ 0.05 in all cases ($p < 0.05$ *, $p < 0.01$ **, $p < 0.001$ ***, $p < 0.0001$ ****, n.s.= not significant). Percent of total always refers to percentage of cells of the specified population relative to total PBMCs.

Immunofluorescence staining in esophageal biopsies

Immunofluorescence staining was performed in biopsies from control subjects and EoE patients, previously oriented in a cellulose acetate and included in paraffin-embedded blocks, using the antibodies CD123-biotin (Stem Cell, 60110BT), HLA-DR (Santa Cruz, sc-53319) and CD11c (Thermo Fisher Scientific, PA535326). Briefly, slides with 4- μ m sections of esophageal biopsies, underwent deparaffinization, antigen retrieval using sodium citrate buffer (pH 6.0), blocked with 4% goat serum/phosphate-buffered saline (PBS), and then incubated with primary antibody (HLA-DR and CD11c) diluted in 1% goat serum-PBS overnight at 4 °C in a humidified chamber. Then, slides were washed with PBS + 1% NP-40 and incubated with secondary antibodies diluted in 1% goat serum-PBS for 30min at RT in a humidified chamber. After, slides were washed with PBS + 1% NP-40 and incubated with primary antibody (CD123) diluted in 1% goat serum/PBS overnight at 4 °C in a humidified chamber. Finally, slides were washed in PBS + 1% NP-40 and incubated with secondary antibodies and DAPI (0.5 μ g/mL) diluted in 1% goat serum/PBS for 30min at RT in a humidified chamber. Finally, a cover slip was added with ProLong Gold mounting reagent (Molecular Probes). Images were obtained using a Thunder Imager (Leica) with LAS X software and analysis was done using ImageJ and RStudio software. Normality was assessed by Saphiro Wilk normality test, the non-parametric Mann-Whitney test was done to compare between pairs of groups. In all cases ($p < 0.05$ *, $p < 0.01$ **, $p < 0.001$ ***, $p < 0.0001$ ****, n.s.= not significant).

RESULTS

Patient Demographics

Clinical and demographic characteristics of study participants are summarized in Table 1. Compared to controls (n=19), EoE patients (n=25) were older (34 vs 41 years) and more frequently male (68% vs 88%), but no significant differences were found in demographic characteristics across groups.

EoE patients treated with PPI (n=18) were classified as responders or non-responders to the therapy. EoE remission was defined as presenting a peak eosinophil count below 15 after at least 8 weeks of treatment. Response to PPI was also associated with improvement in EoE symptoms from baseline (assessed as patient reported outcomes), as well as in endoscopic and histologic characteristics, assessed with the scores EREFS and Grade and Stage EoEHSS, respectively. Baseline characteristics of PPI responding, and non-responding patients showed no differences.

	Control (n=19)	EoE (n=25)	p-value	Responders (n=9)	Non-Responders (n=9)	p-value
Sex (male) (n,%)	13 (68%)	20 (80%)	0.488	7 (77%)	7 (77%)	1
Age (mean years \pm s.d.)	34.42 \pm 10.93	41 \pm 13.7	0.060	33 \pm 12.85	44 \pm 14.95	0.152
Symptoms (n,%)						
Dysphagia	0	23 (92%)	<0.001	9 (100%)	9 (100%)	1
Food impaction	0	16 (64%)	<0.001	7 (77%)	5 (55%)	0.819
Heartburn	0	10 (40%)	0.002	3 (33%)	3 (33%)	1
Abdominal pain	0	0 (0%)	1	0 (0%)	0 (0%)	1
Any atopic disease (n,%)						
Atopic diseases	1 (5%)	20 (87%)	<0.001	8 (88%)	9 (100%)	1
Asthma	0	5 (22%)	0.053	3 (33%)	1 (11%)	0.573
Allergic rhinitis/sinusitis	1 (5%)	19 (82%)	<0.001	8 (88%)	9 (100%)	1
Food allergy	2 (10%)	11 (48%)	0.0173	5 (55%)	3 (33%)	0.637
Endoscopic findings (n,%)						
EREFS (mean \pm s.d.)	0	3.36 \pm 2	<0.001	2.44 \pm 2.06	3.88 \pm 1.26	0.097
EREFS PostPPI (mean \pm s.d.)	-	-	-	1.44 \pm 1.51	4.33 \pm 1	<0.001
Maximum eosinophil count (mean \pm s.d.)	0	55.68 \pm 23.9	<0.001	46.22 \pm 21.76	65.56 \pm 19.43	0.064
Maximum eosinophil count PostPPI (mean \pm s.d.)	-	-	-	1.44 \pm 2	65 \pm 20.91	<0.001
Histological findings						
EoEHSS Grade (0-1) (mean \pm s.d.)	0	0.50 \pm 0.19	<0.001	0.43 \pm 0.22	0.57 \pm 0.15	0.122
EoEHSS Grade (0-1) PostPPI (mean \pm s.d.)	-	-	-	0.06 \pm 0.04	0.40 \pm 0.22	0.006
EoEHSS Stage (0-1) (mean \pm s.d.)	0	0.47 \pm 0.16	<0.001	0.43 \pm 0.17	0.57 \pm 0.15	0.122
EoEHSS Stage (0-1) PostPPI (mean \pm s.d.)	-	-	-	0.02 \pm 0.03	0.31 \pm 0.19	0.007
PPI Treatment						
Omeprazol	-	-	-	6 (66%)	2 (22%)	0.1385
Esomeprazol	-	-	-	2 (22%)	2 (22%)	
Pantoprazol	-	-	-	1 (11%)	5 (55%)	

Table 1. Clinical features of controls and EoE patients. Fisher's test and *t*-test were applied to analyse differences between control and EoE patients and between responders and non-responders. P-value is shown for each comparison. Abbreviations: EoE: Eosinophilic Esophagitis; EoEHSS: Eosinophilic Esophagitis Histologic Scoring System; EREFS: EoE endoscopic reference score; PPI: Proton Pump Inhibitors.

379 **High dimensional analysis on PBMCs from controls and EoE patients**

380 A total of 61 samples (19 controls, 24 patients at disease onset, as well as 9
381 responders and 9 non-responders to PPI after 8-week treatment) were analysed by
382 UMAP identifying four major continents and several smaller islands (Figure 1A). The
383 relative expression of each marker on the UMAP (Supplementary Figure 3) revealed
384 that the main continent on the left represents cytotoxic (CD8⁺) T-cells together with
385 double negative (CD4⁻CD8⁻) T-cells. On the other hand, the main continent on the right
386 is composed of helper (CD4⁺) T-cells. Likewise, the island on the bottom is mainly
387 composed of monocytes, basophils and myeloid antigen presenting cells (APC), while
388 the islands in the middle represent NK cells and $\gamma\delta$ T-cells. B-cells are represented in
389 the top island together with dendritic cells.

390
391 To further refine the analysis, FlowSOM algorithm was applied to find similar cell
392 subsets and separate them into metaclusters in an unsupervised manner (Figure 1B).
393 The overlay of the FlowsSOM clustering on the UMAP representation (Figure 1C)
394 allowed us to perform a more exhaustive analysis, identifying a total of 73 clusters
395 according to surface marker expression as shown in the heatmap (Figure 1D).
396 Supplementary Table 2 shows an in-depth characterization of the phenotype of all
397 clusters, which allowed the identification of 70 of them, since clusters 13, 32 and 33
398 could not be clearly identified. Finally, all clusters were further uploaded into the UMAP
399 (Figure 1E) to determine not only how they relate to each other, but also to display their
400 pseudoevolution.

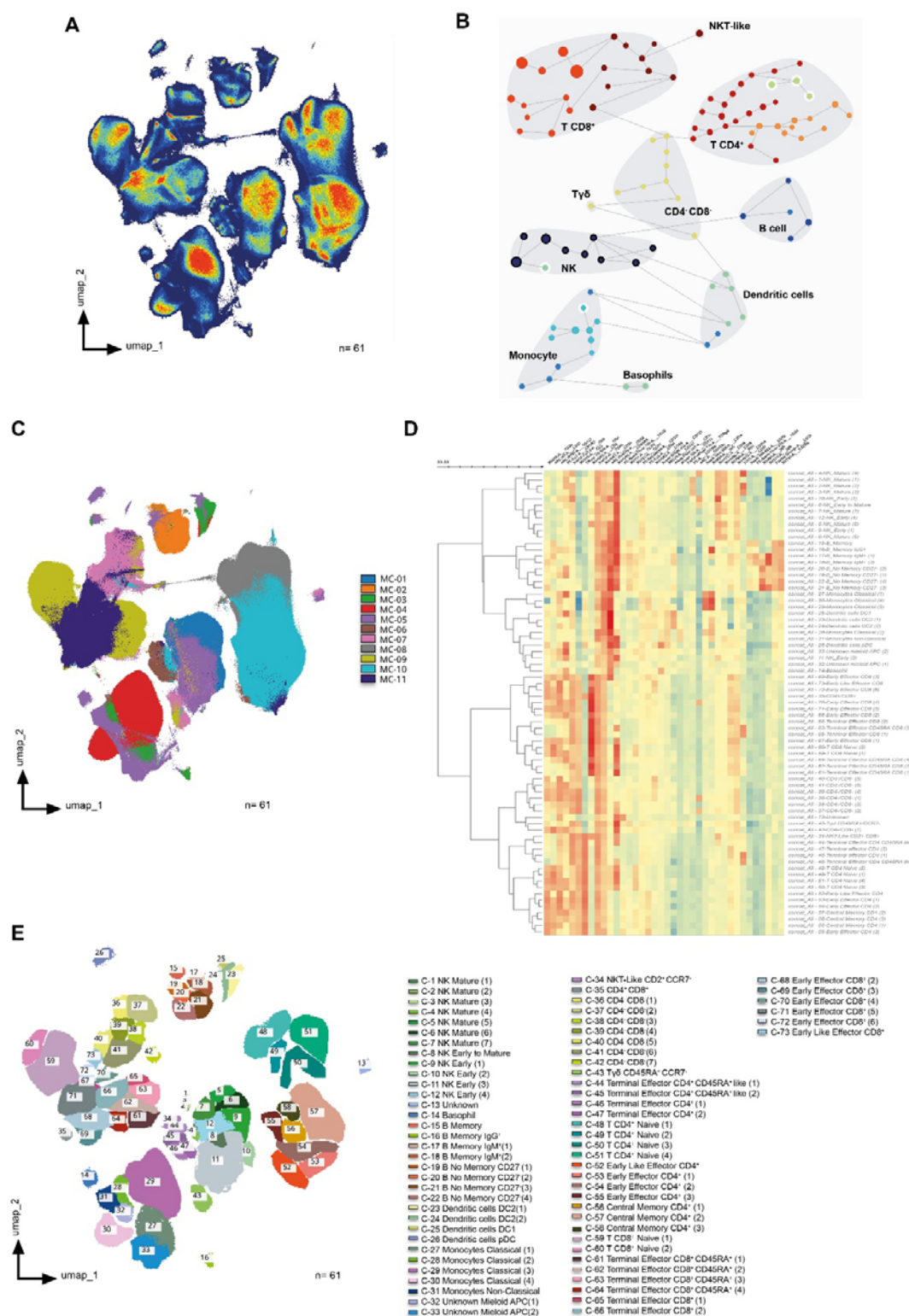


Figure 1. High dimensional analysis of peripheral blood mononuclear cells from controls and EoE patients.

(A) UMAP density analysis representation performed on singlets corresponding to total viable circulating CD45⁺ cells from all samples. Samples were obtained from 19 controls and 24 patients at disease onset, as well as 9 responders and 9 non-

responders to PPI therapy after 8-week treatment (a total of 61 samples). **(B)** FlowSOM clustering on total viable singlet CD45⁺ cells identified the main metaclusters on dataset: B-cells, NK cells, $\gamma\delta$ T-cells, CD4⁺ T-cells, CD8⁺ T-cells, dendritic cells, basophils, monocytes, CD4⁺CD8⁺ T-cells, and NKT-like cells. **(C)** UMAP representation of all samples after non-supervised FlowSOM clusterization **(D)** Heatmap displaying the relative expression of each marker within each of the 73 identified clusters. Euclidean distance between clusters was calculated and represented by the dendrogram at the left side of the plot. **(E)** All 73 identified clusters were overlaid on the UMAP projection. Each identified cluster is tagged by a specific colour and number as shown in the legend.

Peripheral immune profile differs between EoE patients and controls at baseline visit

After characterizing the different clusters, or immune subsets, present in our samples, we next addressed the immune differences found between controls and EoE patients at baseline visit. Volcano plot representation (Figure 2A) showed a significant deficit of plasmacytoid dendritic cells (pDC) (C-26) in EoE patients and an expansion of CD4⁺CD8⁺ and early effector CD8⁺ T-cells (Clusters 37 and 69) at the time of disease diagnosis (Figure 2B). In order to further confirm these findings, classical gating strategies were applied as shown in Supplementary Figure 2, hence confirming that EoE patients display a deficit of circulating pDC at disease onset (Figure 2C).

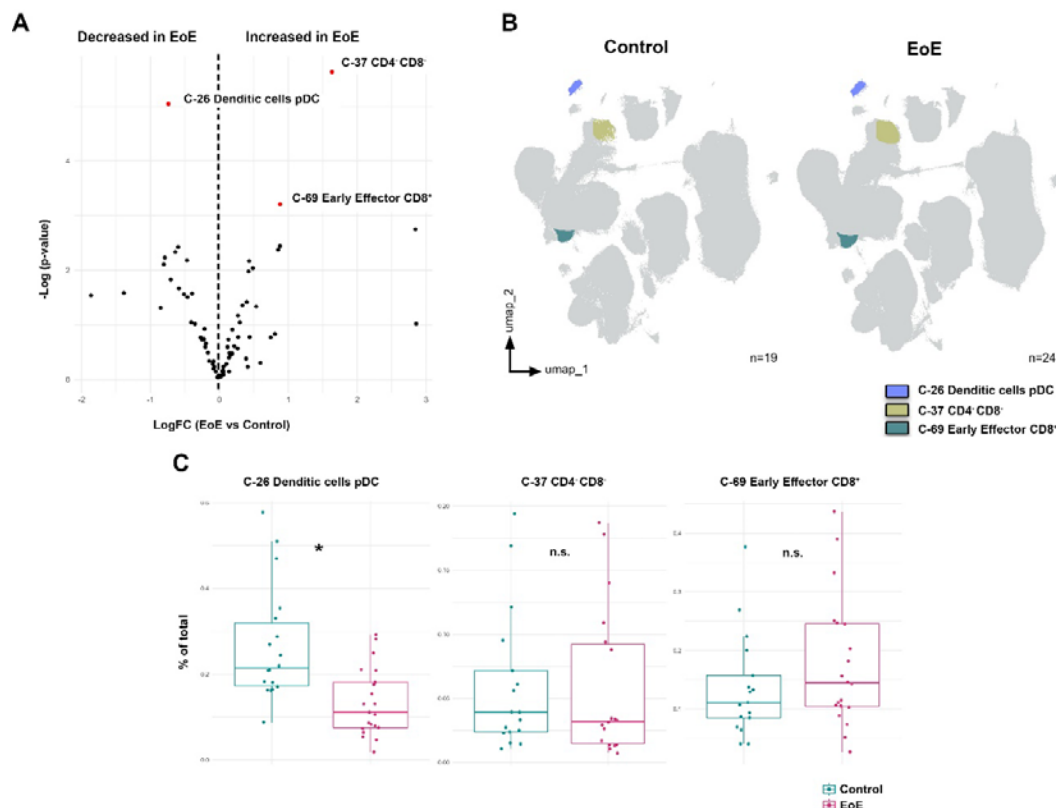


Figure 2. Peripheral immune profile differs between EoE patients and controls at baseline visit.

433 **(A)** Volcano plot analysis comparing clusters from controls (n=19) and patients with
 434 eosinophilic esophagitis at disease diagnosis (EoE, n=24). LogFC and -Log(p-value)
 435 are shown. Clusters considered statistically significant are shown in red together with
 436 their nature as elucidated from Supplementary Table 2. **(B)** These differentially
 437 expressed clusters between control and EoE patients are further shown in the UMAP
 438 representation. **(C)** Validation of these clusters was performed following classical
 439 gating approaches (Supplementary Figure 1 and 2). *t*-test was applied in panel D,
 440 considering a p-value <0.05 as statistically significant (*p<0.05). Percent of total always
 441 refers to percentage of cells of the specified population relative to total PBMCs.

442

443 **Circulating pDC and classical monocyte levels at baseline are associated to PPI**
 444 **response.**

445

446 After describing that 3 clusters were differentially expressed on EoE patients at disease
 447 diagnosis, with a specific reduction of circulating pDCs as confirmed by classical gating
 448 approaches, we next aimed to address whether we could also identify specific clusters
 449 that might predict patient's response to PPI treatment.

450 To that end, we compared the immune profile of responding (R) and non-responding
 451 (NR) patients (Table1) at disease onset (i.e., before PPI treatment [PrePPI]) (Figure
 452 3A). Our results revealed that responding patients at diagnosis had higher levels of
 453 circulating pDC, myeloid antigen presenting cells and classical monocytes; together
 454 with lower levels of mature NK cells, and no memory B-cells and central memory CD4⁺
 455 T-cells (Figures 3B and 3C). Of note, further analysis following classical gating
 456 approaches confirmed that PPI-responding patients had higher levels of circulating
 457 pDC and classical monocytes at disease onset compared to non-responders (Figure
 458 3D).

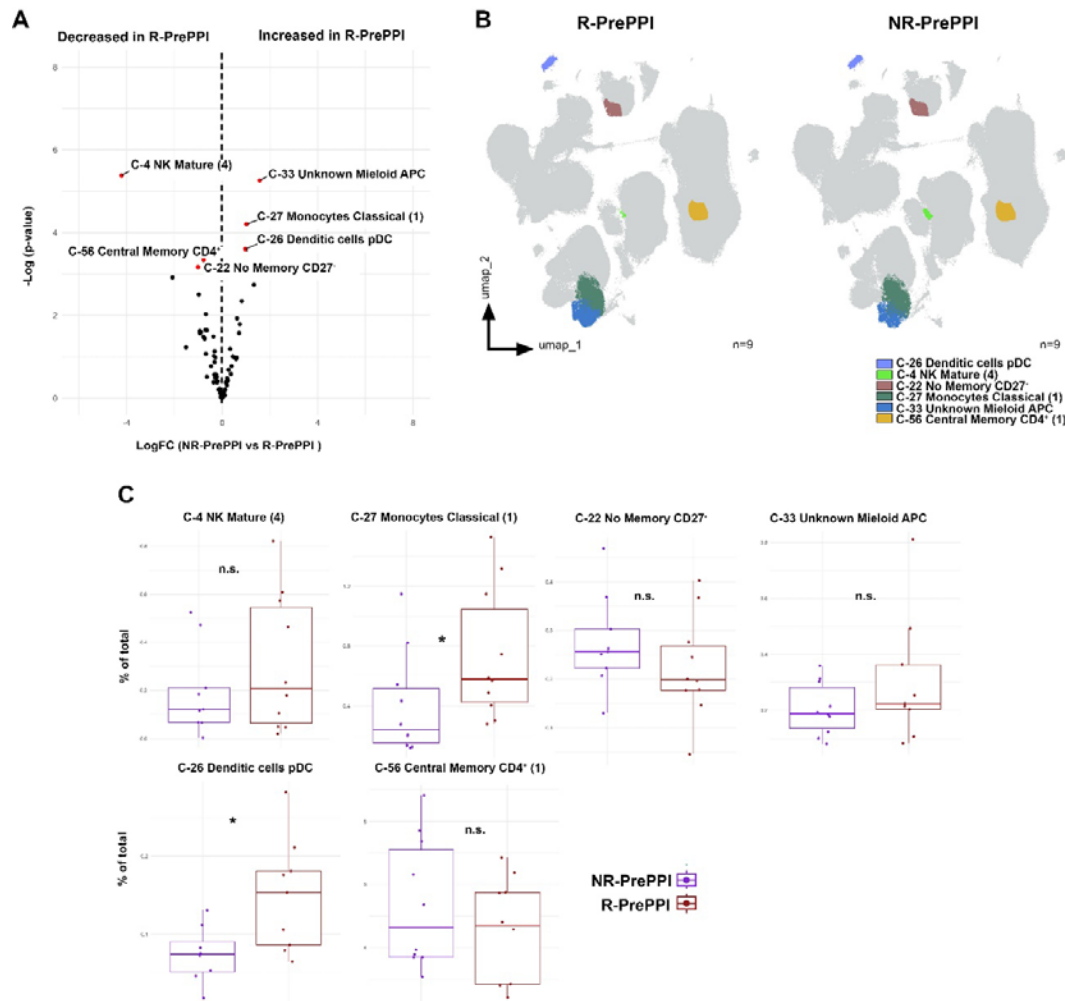


Figure 3. Circulating pDC and classical monocyte levels are associated to PPI response at disease diagnosis

(A) Volcano plot of differential analysis between responding (R, n=9) and non-responding patients (NR, n=9). LogFC and -Log(p-value) at baseline are shown. Clusters considered statistically significant are highlighted in red, showing their name and number. **(B)** UMAP representation from R and NR patients, in which significant clusters are coloured. **(C)** Validation by classic gating (Supplementary Figure 1 and 2) of the significant clusters previously defined. Boxplots of significant clusters represent individual percentage of total value, group medians as well as minimum and maximum values. Differences were analysed by t-test considering p-values <0.05 as statistically significant (*p<0.05, **p<0.01, ***p<0.001, ****p<0.0001) (R n=8, NR n=7). Responder (R), Non-Responder (NR), before treatment (PrePPI). Percent of total always refers to percentage of cells of the specified population relative to total PBMCs.

Circulating pDC levels are restored in PPI-responding patients following treatment

Since patients with PPI responsive and non-responsive EoE displayed different immune cell levels at the time of disease diagnosis, we next aimed to address whether we could also identify specific clusters modulated by PPI treatment. To that end, we

next compared the profile of EoE responsive (R) patients both before (PrePPI) and after (PostPPI) PPI therapy (Table1). Our results revealed that, following treatment, circulating levels of pDC (C-26) and basophils (C-14) were increased in PPI-responding patients (Figures 4A and 4B), something particularly relevant in the case of circulating pDC as that increase was further confirmed by classical gating approaches (Figure 4C). Based on these observations, we also assessed the immune cell dynamics in non-responding patients (Supplementary Figure 4A). The pDC cluster was increased in these patients following treatment (Supplementary Figure 4B); however, that observation could not be confirmed following classical gating strategy (Supplementary Figure 4C). Therefore, taken all together our results suggest that clinical response to PPI-treatment is associated with an increase in circulating pDC levels.

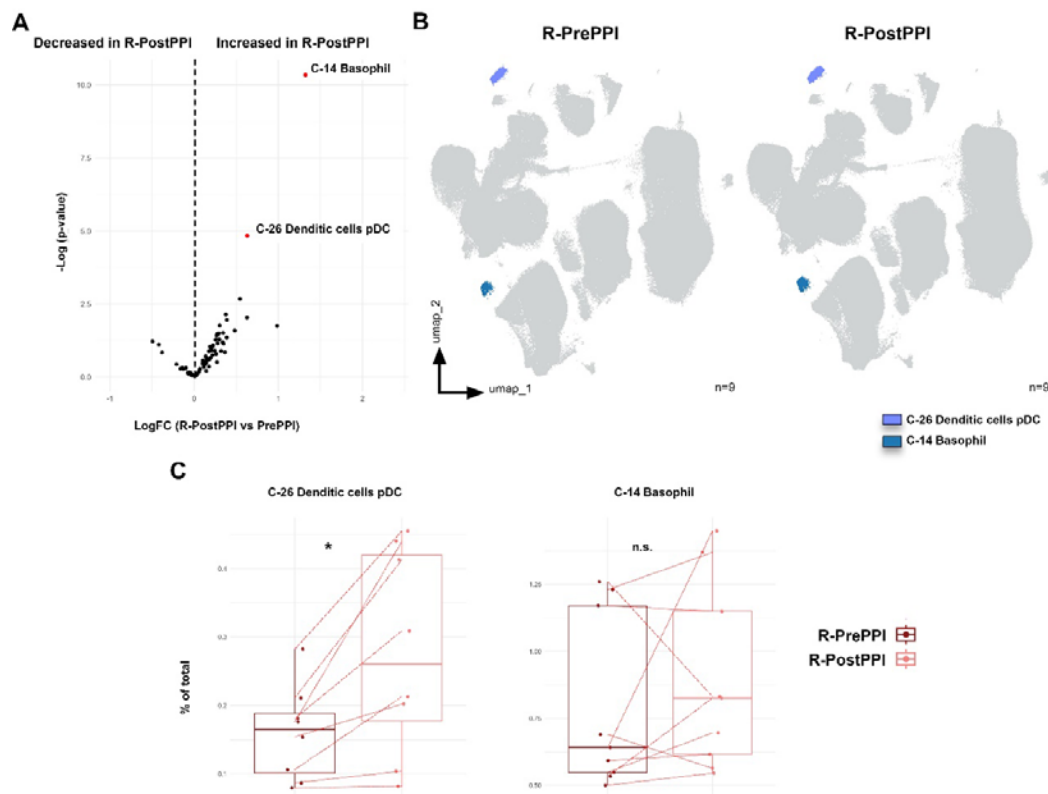


Figure 4. pDC and basophil levels are increased in responding patients upon PPI treatment.

(A) Volcano plot analysis of the clusters comparing patients responding to proton pump inhibitor (PPI) treatment, both before (R-PrePPI) and after (R-PostPPI) therapy. LogFC and -Log(p-value) are shown. Clusters considered statistically significant are shown in red together with their nature as elucidated from Supplementary Table 2. **(B)** UMAP representation of these differentially expressed clusters in R-PrePPI and R-PostPPI. **(C)** Further validation of these clusters was performed following classical gating approaches as shown in Supplementary Figure 1 and 2. Boxplots of significant clusters represent individual percentage of total value, group medians as well as minimum and maximum values. Red line indicates paired PrePPI and PostPPI samples. Differences

were analysed by paired *t*-test considering p-values <0.05 as statistically significant (*p<0.05, **p< 0.01, ***p< 0.001, ****p<0.0001) (n=8). Responder (R), before PPI treatment (PrePPI), after PPI treatment (PostPPI). Percent of total always refers to percentage of cells of the specified population relative to total PBMCs.

Circulating pDCs are associated with EoE pathology and PPI-response

Having described that pDCs are differentially decreased in EoE patients at the moment of diagnosis, (Figure 2) while within EoE patients they are higher in those who respond to PPI treatment (Figure 3) and, indeed, they are further increased following such clinical intervention (Figure 4) although not in non-responding patients (Supplementary Figure 4), we next decided to focus on this cell population. Hence, further analysis confirmed that all EoE patients had lower levels of circulating pDCs at diagnosis, although these levels were lower in non-responding patients than in responders. Furthermore, in responders pDC levels were indeed further restored to control levels following treatment.

Since pDCs seem to be related to disease remission, we next hypothesized that cells might be correlated with the esophageal inflammatory state of the patient. To test this hypothesis, we studied the correlation between the maximum eosinophil count in the esophageal biopsy and pDC levels (Figure 5B). We found a negative correlation ($r = -0.44$ p-value= <0.001), suggesting the implication of pDCs in EoE pathogenesis.

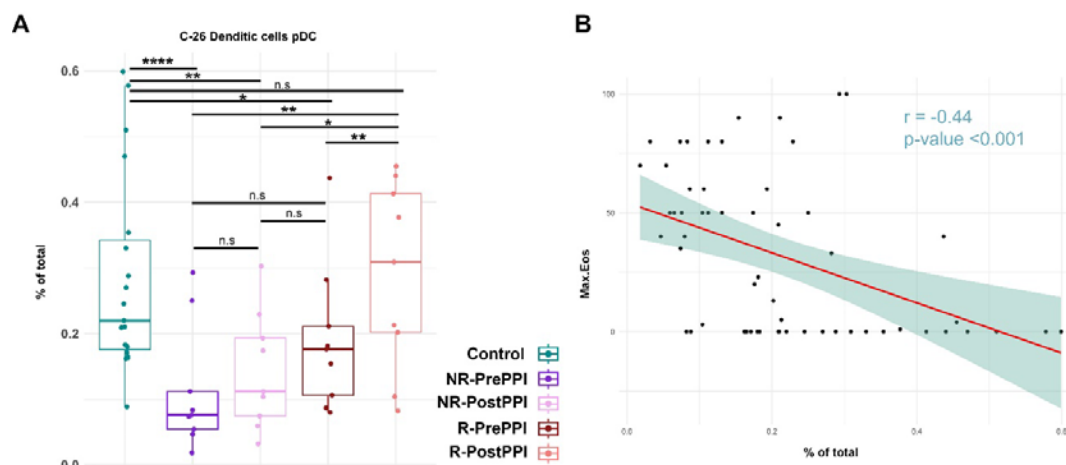


Figure 5. Circulating pDC are associated with EoE pathology and PPI-response
(A) Boxplots represent levels of pDC in control and EoE patients before and after PPI treatment, as individual percentages of total counts as well as group medians and minimum and maximum values. Differences were analysed by *t*-test, considering p-values <0.05 as statistically significant. **(B)** Pearson correlation between pDC and peak eosinophil count. Pearson correlation coefficient and p-value are shown. (Control n=19, R n=9, NR n=9). Responder (R), Non-Responder (NR), before PPI treatment (PrePPI), after PPI treatment (PostPPI) (*p<0.05, **p< 0.01, ***p< 0.001, ****p<0.0001).

542

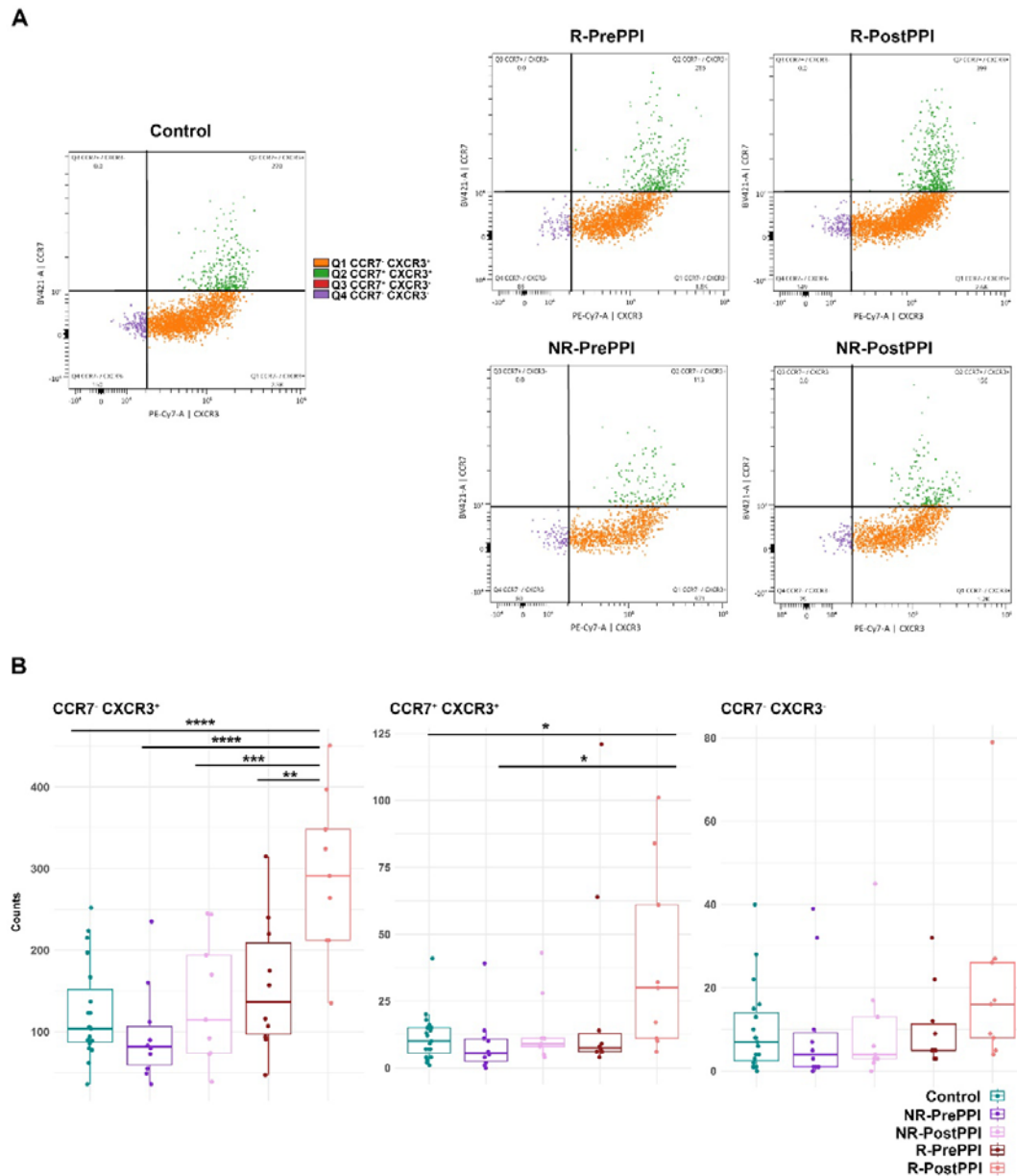
543 Differential activation profile of circulating pDCs in EoE and remission

544

545 Next, we assessed the expression of the chemokine receptors CCR7 and CXCR3 on
546 circulating pDC, as they mediate pDC migration towards the lymph nodes (LN) and
547 peripheral sites of inflammation^{28,29} (Figure 6A). CXCR3⁺ pDC (either CCR7⁺ or CCR7⁻)
548 were increased in PPI responding patients following treatment (Figure 6B) suggesting a
549 potential mechanism of action for pDC related with their infiltration in the esophagus.

550

551



552

553

554 **Figure 6. Differential activation profile of circulating pDC in EoE and remission.**

555 **(A)** Gating of activated pDC subpopulations according to their CCR7 and CXCR3

expression: CCR7⁺/CXCR3⁺ (blue), CCR7⁺/CXCR3⁺ (orange), CCR7⁺/CXCR3⁻ (green), CCR7⁺/CXCR3⁻ (red). Dot plots show representative distribution of these subpopulations in each cohort. **(B)** Boxplot representation of the different pDC activation profiles in the five cohorts. Total count, group median and minimum and maximum values are represented. Differences were analysed by multiple comparison ANOVA followed by *post hoc* Fisher's test, considering p-values <0.05 as statistically significant (*p<0.05, **p< 0.01, ***p< 0.001, ****p<0.0001). (Control n=19, R n=9, NR n=9). Responder (R), Non-Responder (NR), before treatment (PrePPI), after treatment (PostPPI).

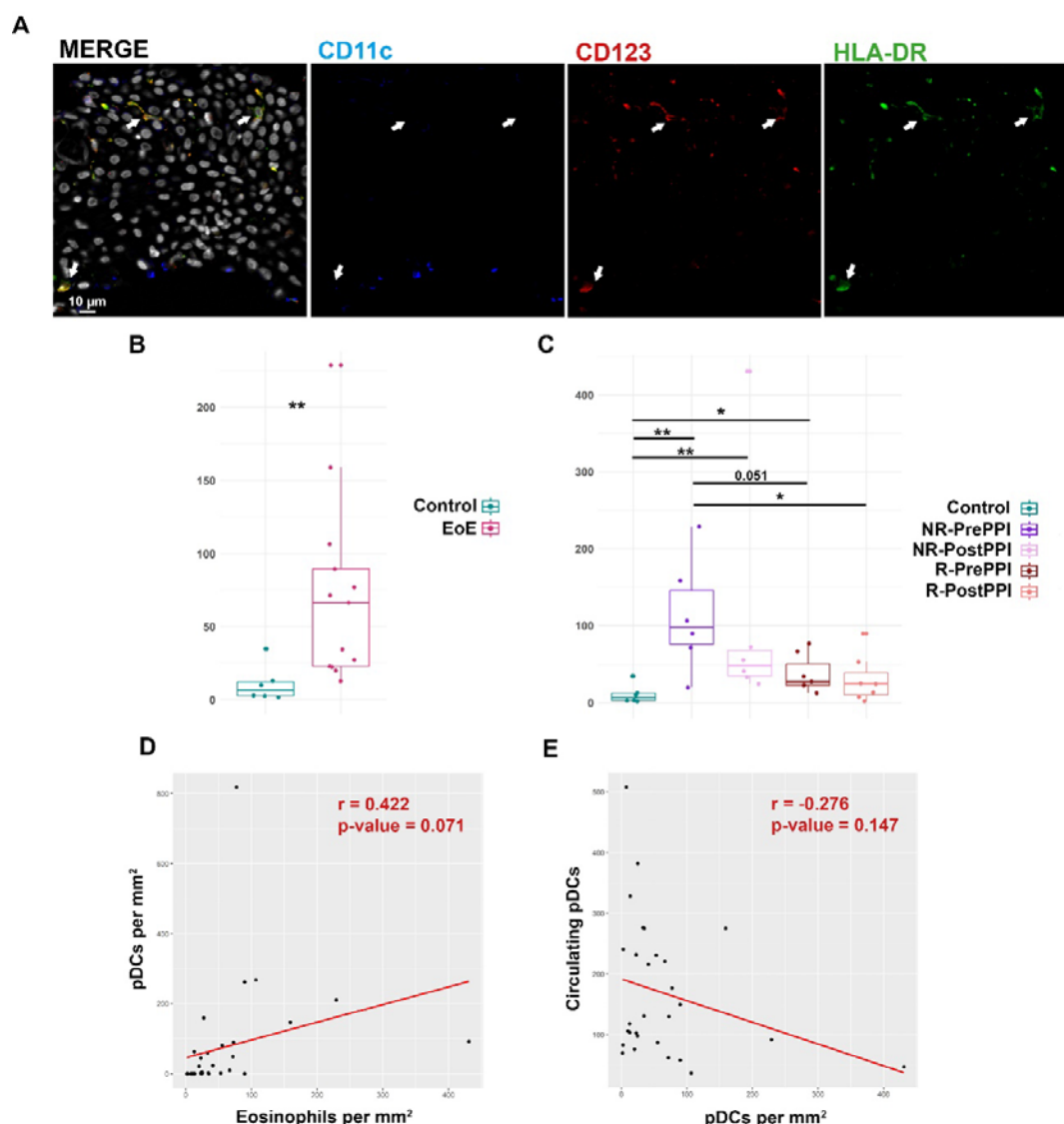
565

566 **pDC infiltration in esophageal biopsies of EoE patients**

567

568 Finally, after describing the activation profile of the circulating pDC population, we
569 studied by immunofluorescence assay the infiltration of these cells in esophageal
570 biopsies of 7 healthy controls and 13 EoE patients (6 R and 7 NR) before and after PPI
571 treatment (Figure 7). pDCs were characterized as CD123⁺ (red) HLA-DR⁺ (green)
572 CD11c⁻ (blue) cells and quantified per mm² of tissue (Figure 7A). The number of tissue
573 pDCs was significantly higher in EoE patients than in controls (Figure 7B), being higher
574 in NR-prePPI when compared to R-prePPI (Figure 7C). The number of tissue pDCs
575 was reduced in NR and R patients after PPI treatment although differences were not
576 statistically significant. However, R-postPPI values were the closest to those of
577 controls (Figure 7C).

578 In general, tissue pDCs inversely correlated with the circulating pDC count and were
579 directly related with the number of eosinophils per mm² (Figure 7D,E). Thus, levels of
580 this immune population seem to be related with PPI-response and EoE activity.



581

582 **Figure 7. pDC infiltration in esophageal biopsies of EoE patients (A)**
 583 Immunofluorescence analysis of pDC infiltrate in esophageal biopsies from EoE
 584 patients. pDCs were visualized as CD123⁺(red) CD11c⁻ (blue), HLA-DR⁺ (green) cells.
 585 Arrows point to representative examples of pDC. Scale bar is shown. Nuclei were
 586 stained with DAPI (represented in grey in merged images). **(B)** Boxplot representation
 587 of infiltrating pDCs in controls (n=7) and EoE (n=13) patients at baseline. Relative
 588 count per mm², group median and minimum and maximum values are represented.
 589 Differences were analysed by Mann-Whitney test, considering p-values <0.05 as
 590 statistically significant (*p<0.05, **p< 0.01, ***p< 0.001, ****p<0.0001). **(C)**
 591 Boxplot representation of infiltrating pDCs in controls (n=7), responder (n=6) and non-
 592 responder (n=7) pre-PPI and post-PPI. Relative count per mm², group median and
 593 minimum and maximum values are represented. Differences were analysed by Mann-
 594 Whitney test, considering p-values <0.05 as statistically significant (*p<0.05, **p< 0.01,
 595 ***p< 0.001, ****p<0.0001). Responder (R), Non-Responder (NR), before treatment
 596 (PrePPI), after treatment (PostPPI). **(D)** Pearson correlation between tissue eosinophil
 597 count and tissue pDCs. Pearson correlation coefficient and p-value are shown. **(E)**

598 Pearson correlation between circulating pDC and tissue pDCs. Pearson correlation
599 coefficient and p-value are shown.
600

601 DISCUSSION

602 Using state-of-the-art spectral cytometry, we hereby describe, for the first time to our
 603 knowledge, a unique fingerprint in the circulating immunome of patients with EoE at the
 604 time of disease diagnosis characterized by a specific deficit of circulating pDCs.
 605 Indeed, their levels were further decreased at diagnosis in patients who did not
 606 respond to PPI treatment, while among those who did, circulating levels of this cell
 607 subset were restored to normal levels upon treatment. Moreover, when we evaluated
 608 the presence of pDCs in the esophagus their numbers correlated with the eosinophilic
 609 count, showing both an inverse correlation with circulating pDCs. Hence, our findings
 610 suggest a central role of pDCs in the pathogenesis of EoE and reveal them as potential
 611 novel non-invasive biomarkers to aid on disease diagnosis and predict subsequent
 612 response to PPI therapy.

613 In addition to our novel findings on pDCs, we found an increase in CD4⁺CD8⁻ T-cells
 614 and CD8⁺ Early Effectors (C-37 and C-69, respectively) in EoE patients at diagnosis,
 615 although these results could not be further confirmed by classical gating approaches.
 616 Increased levels of T-cells could be related with the active role of CD8⁺T cells in the
 617 esophageal inflammation in EoE^{30,31} while the change in CD4⁺CD8⁻ T-cells might be
 618 associated with their cytotoxic activity as described for other pathologies³², despite no
 619 role for these cells has been found in EoE.

620 PPI therapy is widely used in the management of EoE^{16,33}, with a histologic remission
 621 rate of approximately 50%¹⁶. The reduction in Th2 signalling produced by this therapy
 622 leads to an improvement in the structural characteristics of the esophagus,
 623 accompanied by decreased eosinophil count. In our study, non-responding patients
 624 presented significant differences from responding patients (Figure 3A). When we
 625 studied these two groups PrePPI intake, non-responding patients had lower levels of
 626 pDCs, classical monocytes and an unknown myeloid APC cluster, but higher levels of
 627 non-memory B cells, mature NK cells and central memory CD4⁺ T-cells. These results
 628 might indicate an increased antigen presentation activity, since they have decreased
 629 numbers of circulating APC populations, which are key in homeostasis and allergy
 630 response³⁴. Indeed, latest results from our group³⁵ reinforce this hypothesis showing
 631 that non-responding patients' esophageal proteomic profile when compared to
 632 responding patients (both PrePPI), have increased levels of proteins associated with
 633 antigen presentation. These patients might have a more altered barrier in the
 634 esophagus, which increases the risk of antigen exposure, thereby favouring EoE
 635 worsening, as described before³⁶⁻³⁸. Although these findings need a deeper
 636 characterization, they unveil for the first time a differential immunological profile
 637 between patients that will or will not respond to PPI therapy and could open the door to
 638 a better profiling of refractory patients.

639 In addition, when we studied immune dynamics during PPI treatment, PPI-responding
 640 patients displayed a significant increase in circulating basophils (C-14) and pDCs (C-
 641 26) (Figure 4A). Basophils have a pivotal role in atopic diseases and are a major
 642 source of Th2 immunomodulation. The increased levels of these cells in patients who
 643 achieve remission after PPI therapy could be related to the reestablishment of
 644 immunological homeostasis, since during inflammation basophils are able to penetrate
 645 the inflamed esophagus³⁹. A similar role may be played by circulating pDCs, which
 646 recover control values in PPI-responding patients PostPPI (Figure 5A). pDCs produce
 647 high levels of IFN- $\alpha\beta$ (type I). This cytokine impairs Th2 responses by blocking the

normal development of Th2 cells and production of Th2 cytokines (especially IL-5)^{40,41}. The reduction in circulating pDCs during active esophageal inflammation could be indicating migration of these cells to the inflamed tissue to control the inflammatory response. Conceivably, circulating levels of these cells are restored when the patient achieves remission. Importantly, the chemokine receptors CXCR3 and CCR7 related to pDC migration to tissues and homing to the LN^{28,29,42} were expressed in circulating pDCs (Figure 6A) in our cohorts. Indeed, responders presented the most activated pDCs after PPI treatment (Figure 5B) while no significant changes were found in the case of non-responding patients. Together with the previous results, the observed low levels of pDCs in PrePPI and PostPPI non-responding patients (Figure 5A) and their less active circulating profile (Figure 6B), could be linked to a poor inhibition of the Th2 response by type I IFN or/and a more exacerbated mucosal barrier alteration and therefore a worse prognosis^{36,40}. Focusing on promising minimally invasive biomarkers, pDCs are a potentially interesting candidate since they are highly related with EoE onset and the response to treatment. We have observed an inverse correlation between circulating pDCs and the peak eosinophil count in esophageal biopsies (Figure 5B). Moreover, when we evaluated tissue pDC levels in patient's biopsies we found a positive correlation between these cells and the proportion of eosinophils per mm² (Figure 7D), being also inversely correlated to pDC circulating levels (Figure 7E). In patients, the number of tissue pDCs was higher when the esophageal inflammation was active, reducing their abundance when the inflammation was under control (Figure 7C). However, Responder patients do not reach control values after treatment despite pDC levels tend to be lower. This could be due to a non-complete recovery state, in which these cells participate in the restoration of the esophageal homeostasis as happens in other pathologies⁴³ where tissue healing plays a key role. Thus, it may be that the evaluation of tissue pDC levels in long-term recovered patients would reveal closer numbers to the control. Hence, this population is related with the inflammatory status of the esophagus, thus providing information of clinical diagnostic parameters that until now can only be measured through invasive procedures. In peripheral blood, previous works have related an increase in Th2 profile to active EoE⁴⁴, while others have associated this to eosinophil phenotype or maturation state^{45,46}. Also, single cell studies have described T-cell heterogeneity in the inflamed tissue, defining a specific enrichment in resident CD4⁺ T regulatory and Th2 effector cells together with an increased CD4⁺/CD8⁺ circulating T-cell ratio⁴⁷. Nevertheless, none of these parameters is being used as biomarker for EoE diagnosis, or for the prediction of response to PPI treatment, for which the peripheral eosinophil count has been proposed as a possible predictor⁴⁸. We are aware that advances in biomarker discovery in EoE are hampered by several pitfalls, such as the common concurrence of atopic diseases and the dissociation between the esophageal inflammation and patient's symptoms²³. Accordingly, despite our cohorts are highly controlled and paired samples from the same patients were analysed, further studies and validations are needed to confirm the utility of circulating pDCs as biomarker. The activity of this cluster must be compared in cohorts with other allergic and atopic conditions, since in these pathologies a decreased peripheral pDC count was found, together with pDC infiltration in the inflamed tissue⁴⁹⁻⁵¹. Probably, its visualization through classic cytometry approaches and its combination with other non-

invasive clinical parameters would be helpful to establish a specific signature for EoE management and PPI response prediction, also opening the door to study its utility in the case of other therapy options for EoE.

In summary, we have described, for the first time to our knowledge, the circulating immunome of EoE patients at the time of diagnosis highlighting as well the differences between PPI-responding and non-responding patients. Altogether, our study provides new insights on EoE immunity and sheds light on the characterization of this disorder, proposing a potential biomarker for diagnosis and prediction of response to treatment, which could improve decisions on better treatment options.

REFERENCES

1. Navarro, P., Arias, Á., Arias-González, L., Laserna-Mendieta, E.J., Ruiz-Ponce, M., and Lucendo, A.J. (2019). Systematic review with meta-analysis: the growing incidence and prevalence of eosinophilic oesophagitis in children and adults in population-based studies. *Aliment Pharmacol Ther* 49, 1116–1125. 10.1111/APT.15231.
2. Arias, Á., and Lucendo, A.J. (2019). Incidence and prevalence of eosinophilic oesophagitis increase continuously in adults and children in Central Spain: A 12-year population-based study. *Dig Liver Dis* 51, 55–62. 10.1016/J.DLD.2018.07.016.
3. Lucendo, A.J., Molina-Infante, J., Arias, Á., von Arnim, U., Bredenoord, A.J., Bussmann, C., Amil Dias, J., Bove, M., González-Cervera, J., Larsson, H., et al. (2017). Guidelines on eosinophilic esophagitis: evidence-based statements and recommendations for diagnosis and management in children and adults. *United European Gastroenterol J* 5, 335–358. 10.1177/2050640616689525.
4. Hirano, I., Chan, E.S., Rank, M.A., Sharaf, R.N., Stollman, N.H., Stukus, D.R., Wang, K., Greenhawt, M., Falck-Ytter, Y.T., Chachu, K.A., et al. (2020). AGA Institute and the Joint Task Force on Allergy-Immunology Practice Parameters Clinical Guidelines for the Management of Eosinophilic Esophagitis. *Gastroenterology* 158, 1776–1786. 10.1053/J.GASTRO.2020.02.038.
5. Schoepfer, A., and Safroneeva, E. (2014). Activity assessment of eosinophilic esophagitis. *Dig Dis* 32, 98–101. 10.1159/000357081.
6. McCormick, J.P., and Lee, J.T. (2021). Insights into the Implications of Coexisting Type 2 Inflammatory Diseases. *J Inflamm Res* 14, 4259–4266. 10.2147/JIR.S311640.
7. González-Cervera, J., Arias, Á., Redondo-González, O., Cano-Mollinedo, M.M., Terreehorst, I., and Lucendo, A.J. (2017). Association between atopic manifestations and eosinophilic esophagitis: A systematic review and meta-analysis. *Annals of Allergy, Asthma and Immunology* 118, 582-590.e2. 10.1016/j.anai.2017.02.006.
8. Greuter, T., Alexander, J.A., Straumann, A., and Katzka, D.A. (2018). Diagnostic and Therapeutic Long-term Management of Eosinophilic Esophagitis—Current Concepts and Perspectives for Steroid Use. *Clin Transl Gastroenterol* 9. 10.1038/S41424-018-0074-8.
9. Molina-Infante, J., and Lucendo, A.J. (2017). Proton Pump Inhibitor Therapy for Eosinophilic Esophagitis: A Paradigm Shift. *Am J Gastroenterol* 112, 1770–1773. 10.1038/AJG.2017.404.

- 739 10. Laserna-Mendieta, E.J., Casabona, S., Savarino, E., Perelló, A., Pérez-Martínez, I.,
740 Guagnozzi, D., Barrio, J., Guardiola, A., Asensio, T., de la Riva, S., et al. (2020). Efficacy of
741 Therapy for Eosinophilic Esophagitis in Real-World Practice. *Clin Gastroenterol Hepatol*
742 *18*, 2903-2911.e4. 10.1016/J.CGH.2020.01.024.
- 743 11. Molina-Infante, J., and Lucendo, A.J. (2020). Approaches to diet therapy for eosinophilic
744 esophagitis. *Curr Opin Gastroenterol* *36*, 359–363. 10.1097/MOG.0000000000000645.
- 745 12. Molina-Infante, J., Bredenoord, A.J., Cheng, E., Dellon, E.S., Furuta, G.T., Gupta, S.K.,
746 Hirano, I., Katzka, D.A., Moawad, F.J., Rothenberg, M.E., et al. (2016). Proton pump
747 inhibitor-responsive oesophageal eosinophilia: an entity challenging current diagnostic
748 criteria for eosinophilic oesophagitis. *Gut* *65*, 521–531. 10.1136/GUTJNL-2015-310991.
- 749 13. Dellon, E.S., Rothenberg, M.E., Collins, M.H., Hirano, I., Chehade, M., Bredenoord, A.J.,
750 Lucendo, A.J., Spergel, J.M., Aceves, S., Sun, X., et al. (2022). Dupilumab in Adults and
751 Adolescents with Eosinophilic Esophagitis. *N Engl J Med* *387*, 2317–2330.
752 10.1056/NEJMOA2205982.
- 753 14. Uchida, A.M., Burk, C.M., Rothenberg, M.E., Furuta, G.T., and Spergel, J.M. (2023).
754 Recent advances in the treatment of eosinophilic esophagitis. *J Allergy Clin Immunol*
755 *Pract O*. 10.1016/j.jaip.2023.06.035.
- 756 15. Laserna-Mendieta, E.J., Navarro, P., Casabona-Francés, S., Savarino, E. V., Pérez-
757 Martínez, I., Guagnozzi, D., Barrio, J., Perello, A., Guardiola-Arévalo, A., Betoré-Glaria,
758 M.E., et al. (2023). Differences between childhood- and adulthood-onset eosinophilic
759 esophagitis: An analysis from the EoE connect registry. *Dig Liver Dis* *55*, 350–359.
760 10.1016/J.DLD.2022.09.020.
- 761 16. Laserna-Mendieta, E.J., Casabona, S., Guagnozzi, D., Savarino, E., Perelló, A., Guardiola-
762 Arévalo, A., Barrio, J., Pérez-Martínez, I., Lund Krarup, A., Alcedo, J., et al. (2020).
763 Efficacy of proton pump inhibitor therapy for eosinophilic oesophagitis in 630 patients:
764 results from the EoE connect registry. *Aliment Pharmacol Ther* *52*, 798–807.
765 10.1111/APT.15957.
- 766 17. Van Rhijn, B.D., Warners, M.J., Curvers, W.L., Van Lent, A.U., Bekkali, N.L., Takkenberg,
767 R.B., Kloek, J.J., Bergman, J.J.G.H.M., Fockens, P., and Bredenoord, A.J. (2014).
768 Evaluating the endoscopic reference score for eosinophilic esophagitis: moderate to
769 substantial intra- and interobserver reliability. *Endoscopy* *46*, 1049–1055. 10.1055/S-
770 0034-1377781.
- 771 18. Lucendo, A.J., and Molina-Infante, J. (2016). Limitation of Symptoms as Predictors of
772 Remission in Eosinophilic Esophagitis: The Need to Go Beyond Endoscopy and
773 Histology. *Gastroenterology* *150*, 547–549. 10.1053/J.GASTRO.2016.01.014.
- 774 19. Wen, T., Stucke, E.M., Grotjan, T.M., Kemme, K.A., Abonia, J.P., Putnam, P.E., Franciosi,
775 J.P., Garza, J.M., Kaul, A., King, E.C., et al. (2013). Molecular diagnosis of eosinophilic
776 esophagitis by gene expression profiling. *Gastroenterology* *145*, 1289–1299.
777 10.1053/J.GASTRO.2013.08.046.
- 778 20. Rochman, M., Wen, T., Kotliar, M., Dexheimer, P.J., Morgenstern, N.B.B., Caldwell, J.M.,
779 Lim, H.W., and Rothenberg, M.E. (2022). Single-cell RNA-Seq of human esophageal

780 epithelium in homeostasis and allergic inflammation. *JCI Insight* 7.
781 10.1172/JCI.INSIGHT.159093.

782 21. Rochman, M., Azouz, N.P., and Rothenberg, M.E. (2018). Epithelial origin of eosinophilic
783 esophagitis. *Journal of Allergy and Clinical Immunology* 142, 10–23.
784 10.1016/J.JACI.2018.05.008.

785 22. Molina-Jiménez, F., Ugalde-Triviño, L., Arias-González, L., Relaño-Rupérez, C., Casabona,
786 S., Pérez-Fernández, M.T., Martín-Domínguez, V., Fernández-Pacheco, J.,
787 Laserna-Mendieta, E.J., Muñoz-Hernández, P., et al. (2023). Proteomic analysis of the
788 esophageal epithelium reveals key features of eosinophilic esophagitis
789 pathophysiology. *Allergy*. 10.1111/ALL.15779.

790 23. Rossi, C.M., Lenti, M.V., and Di Sabatino, A. (2022). The need for a reliable non-invasive
791 diagnostic biomarker for eosinophilic oesophagitis. *Lancet Gastroenterol Hepatol* 7,
792 202–203. 10.1016/S2468-1253(21)00468-4.

793 24. Hirano, I., Moy, N., Heckman, M.G., Thomas, C.S., Gonsalves, N., and Achem, S.R.
794 (2013). Endoscopic assessment of the oesophageal features of eosinophilic
795 oesophagitis: validation of a novel classification and grading system. *Gut* 62, 489–495.
796 10.1136/GUTJNL-2011-301817.

797 25. Collins, M.H., Martin, L.J., Alexander, E.S., Todd Boyd, J., Sheridan, R., He, H., Pentiuik,
798 S., Putnam, P.E., Abonia, J.P., Mukkada, V.A., et al. (2017). Newly developed and
799 validated eosinophilic esophagitis histology scoring system and evidence that it
800 outperforms peak eosinophil count for disease diagnosis and monitoring. *Dis Esophagus*
801 30. 10.1111/DOTE.12470.

802 26. Park, L.M., Lannigan, J., and Jaimes, M.C. (2020). OMIP-069: Forty-Color Full Spectrum
803 Flow Cytometry Panel for Deep Immunophenotyping of Major Cell Subsets in Human
804 Peripheral Blood. *Cytometry A* 97, 1044–1051. 10.1002/CYTO.A.24213.

805 27. McInnes, L., Healy, J., Saul, N., and Großberger, L. (2018). UMAP: Uniform Manifold
806 Approximation and Projection. *J Open Source Softw* 3, 861. 10.21105/JOSS.00861.

807 28. Vanbervliet, B., Bendriss-Vermare, N., Massacrier, C., Homey, B., De Bouteiller, O.,
808 Brière, F., Trinchieri, G., and Caux, C. (2003). The Inducible CXCR3 Ligands Control
809 Plasmacytoid Dendritic Cell Responsiveness to the Constitutive Chemokine Stromal
810 Cell–derived Factor 1 (SDF-1)/CXCL12. *J Exp Med* 198, 823. 10.1084/JEM.20020437.

811 29. Seth, S., Oberdörfer, L., Hyde, R., Hoff, K., Thies, V., Worbs, T., Schmitz, S., and Förster,
812 R. (2011). CCR7 Essentially Contributes to the Homing of Plasmacytoid Dendritic Cells to
813 Lymph Nodes under Steady-State As Well As Inflammatory Conditions. *The Journal of*
814 *Immunology* 186, 3364–3372. 10.4049/JIMMUNOL.1002598.

815 30. Anilkumar, A.A., Beppu, L., Kurten, R., Newbury, R., Dohil, R., Broide, D., and Aceves,
816 S.S. (2014). CD3 and CD8 Cells Produce IL-9 In Pediatric Eosinophilic Esophagitis. *Journal*
817 *of Allergy and Clinical Immunology* 133, AB288. 10.1016/j.jaci.2013.12.1017.

818 31. Abdolahi, M., Rasouli, S., Babaie, D., Dara, N., Imanzadeh, F., Sayyari, A., Rouhani, P.,
819 Khatami, K., Kazemiaghdam, M., Nilipour, Y., et al. (2021). Increased regulatory T cells in
820 peripheral blood of children with eosinophilic esophagitis. *Gastroenterol Hepatol Bed*
821 *Bench* 14, 25–30.

- 822 32. Wu, Z., Zheng, Y., Sheng, J., Han, Y., Yang, Y., Pan, H., and Yao, J. (2022). CD3+CD4-CD8-
823 (Double-Negative) T Cells in Inflammation, Immune Disorders and Cancer. *Front*
824 *Immunol* 13, 388. 10.3389/FIMMU.2022.816005/BIBTEX.
- 825 33. Chang, J.W., Saini, S.D., Mellinger, J.L., Chen, J.W., Zikmund-Fisher, B.J., and Rubenstein,
826 J.H. (2019). Management of eosinophilic esophagitis is often discordant with guidelines
827 and not patient-centered: results of a survey of gastroenterologists. *Dis Esophagus* 32.
828 10.1093/DOTE/DOY133.
- 829 34. Schülke, S., Gilles, S., Jirno, A.C., and Mayer, J.U. (2023). Tissue-specific
830 antigen-presenting cells contribute to distinct phenotypes of allergy. *Eur J Immunol*,
831 2249980. 10.1002/EJI.202249980.
- 832 35. Molina-Jiménez, F., Ugalde-Triviño, L., Arias-González, L., Relaño-Rupérez, C., Casabona,
833 S., Moreno-Monteagudo, J.A., Pérez-Fernández, M.T., Martín-Domínguez, V.,
834 Fernández-Pacheco, J., Laserna-Mendieta, E.J., et al. (2023). Proton pump Inhibitor
835 effect on esophageal protein signature of eosinophilic esophagitis, prediction and
836 evaluation of treatment response. *medRxiv*, 2023.11.21.23298292.
837 10.1101/2023.11.21.23298292.
- 838 36. Chen, J., Oshima, T., Huang, X., Tomita, T., Fukui, H., and Miwa, H. (2022). Esophageal
839 Mucosal Permeability as a Surrogate Measure of Cure in Eosinophilic Esophagitis. *J Clin*
840 *Med* 11. 10.3390/JCM11144246.
- 841 37. Furuta, G.T., Fillon, S.A., Williamson, K.M., Robertson, C.E., Stevens, M.J., Aceves, S.S.,
842 Arva, N.C., Chehade, M., Collins, M.H., Davis, C.M., et al. (2023). Mucosal Microbiota
843 Associated With Eosinophilic Esophagitis and Eosinophilic Gastritis. *J Pediatr*
844 *Gastroenterol Nutr* 76, 347–354. 10.1097/MPG.0000000000003685.
- 845 38. Kleuskens, M.T.A., Bek, M.K., Al Halabi, Y., Blokhuis, B.R.J., Diks, M.A.P., Haasnoot, M.L.,
846 Garssen, J., Bredenoord, A.J., C.A.M. van Esch, B., and Redegeld, F.A. (2023). Mast cells
847 disrupt the function of the esophageal epithelial barrier. *Mucosal Immunol*.
848 10.1016/J.MUCIMM.2023.06.001.
- 849 39. Marković, I., and Savvides, S.N. (2020). Modulation of Signaling Mediated by TSLP and
850 IL-7 in Inflammation, Autoimmune Diseases, and Cancer. *Front Immunol* 11.
851 10.3389/FIMMU.2020.01557.
- 852 40. Pritchard, A.L., Carroll, M.L., Burel, J.G., White, O.J., Phipps, S., and Upham, J.W. (2012).
853 Innate IFNs and Plasmacytoid Dendritic Cells Constrain Th2 Cytokine Responses to
854 Rhinovirus: A Regulatory Mechanism with Relevance to Asthma. *The Journal of*
855 *Immunology* 188, 5898–5905. 10.4049/JIMMUNOL.1103507.
- 856 41. Lin, J.Y., Wu, W.H., Chen, J.S., Liu, I.L., Chiu, H.L., Chen, H.W., Tsai, T.L., Huang, Y.L., and
857 Wang, L.F. (2020). Plasmacytoid dendritic cells suppress Th2 responses induced by
858 epicutaneous sensitization. *Immunol Cell Biol* 98, 215–228. 10.1111/IMCB.12315.
- 859 42. Kohrgruber, N., Gröger, M., Meraner, P., Kriehuber, E., Petzelbauer, P., Brandt, S.,
860 Stingl, G., Rot, A., and Maurer, D. (2004). Plasmacytoid Dendritic Cell Recruitment by
861 Immobilized CXCR3 Ligands. *The Journal of Immunology* 173, 6592–6602.
862 10.4049/JIMMUNOL.173.11.6592.

- 863 43. Gregorio, J., Meller, S., Conrad, C., Di Nardo, A., Homey, B., Lauerma, A., Arai, N., Gallo,
864 R.L., DiGiovanni, J., and Gilliet, M. (2010). Plasmacytoid dendritic cells sense skin injury
865 and promote wound healing through type I interferons. *J Exp Med* 207, 2921.
866 10.1084/JEM.20101102.
- 867 44. Adel-Patient, K., Campeotto, F., Grauso, M., Guillon, B., Moroldo, M., Venot, E.,
868 Dietrich, C., Machavoine, F., Castelli, F.A., Fenaille, F., et al. (2023). Assessment of local
869 and systemic signature of eosinophilic esophagitis (EoE) in children through multi-omics
870 approaches. *Front Immunol* 14. 10.3389/FIMMU.2023.1108895.
- 871 45. Perez-Lucendo, I., Gomez Torrijos, E., Donado, P., Melero, R., Feo-Brito, F., and Urra,
872 J.M. (2021). Low Expression of ICAM-1 in Blood Eosinophils in Patients With Active
873 Eosinophilic Esophagitis. *J Investig Allergol Clin Immunol* 31, 316–321.
874 10.18176/JIACI.0489.
- 875 46. Henderson, A., Magier, A., Schwartz, J.T., Martin, L.J., Collins, M.H., Putnam, P.E.,
876 Mukkada, V.A., Abonia, J.P., Rothenberg, M.E., and Fulkerson, P.C. (2020). Monitoring
877 Eosinophilic Esophagitis Disease Activity With Blood Eosinophil Progenitor Levels. *J*
878 *Pediatr Gastroenterol Nutr* 70, 482–488. 10.1097/MPG.0000000000002583.
- 879 47. Wen, T., Aronow, B.J., Rochman, Y., Rochman, M., Kiran, K.C., Dexheimer, P.J., Putnam,
880 P., Mukkada, V., Foote, H., Rehn, K., et al. (2019). Single-cell RNA sequencing identifies
881 inflammatory tissue T cells in eosinophilic esophagitis. *J Clin Invest* 129, 2014–2028.
882 10.1172/JCI125917.
- 883 48. Alexander, R., Alexander, J.A., Akambase, J., Harmsen, W.S., Geno, D., Tholen, C.,
884 Katzka, D.A., and Ravi, K. (2021). Proton Pump Inhibitor Therapy in Eosinophilic
885 Esophagitis: Predictors of Nonresponse. *Dig Dis Sci* 66, 3096–3104. 10.1007/S10620-
886 020-06633-4.
- 887 49. Albanesi, C., Scarponi, C., Pallotta, S., Daniele, R., Bosio, D., Madonna, S., Fortugno, P.,
888 Gonzalvo-Feo, S., Franssen, J.D., Parmentier, M., et al. (2009). Chemerin expression
889 marks early psoriatic skin lesions and correlates with plasmacytoid dendritic cell
890 recruitment. *J Exp Med* 206, 249–258. 10.1084/JEM.20080129.
- 891 50. Saadeh, D., Kurban, M., and Abbas, O. (2016). Update on the role of plasmacytoid
892 dendritic cells in inflammatory/autoimmune skin diseases. *Exp Dermatol* 25, 415–421.
893 10.1111/EXD.12957.
- 894 51. Charles, J., Chaperot, L., Salameire, D., Domizio, J. Di, Aspor, C., Gressin, R., Jacob, M.-
895 C., Richard, M.-J., Beani, J.-C., Plumas, J., et al. (2010). Plasmacytoid dendritic cells and
896 dermatological disorders: focus on their role in autoimmunity and cancer. *Eur J*
897 *Dermatol* 20, 16. 10.1684/EJD.2010.0816.

898

899 **Supplementary Figure 1.** Hierarchical gating strategy for cluster classification.
900 Representative gating strategy used to identify the main leukocyte populations within
901 total peripheral blood mononuclear cells (PBMC). Arrows and gates are used to
902 visualize the relationships across plots. After doublets and dead cells were excluded,
903 basophils were identified as CD45+CD123+CD38+ cells. Monocytes were gated based
904 on FSC-A/SSC-A properties and further classified into non-classical (CD14–CD16+),

intermediate (CD14+CD16+/low), and classical (CD14+CD16-). Within the lymphocyte gate, T-cells were identified based on the expression of CD3. Total $\gamma\delta$ T-cells were identified as CD3+ $\gamma\delta$ T-cell receptor (TCR)+ and subdivided based on the expression of CD45RA and CCR7. Total NKT-like cells were identified in the CD3+ $\gamma\delta$ TCR- compartment as CD56+. The inclusion of CD2 and CD8 further classified the NKT-like cells. Total T-cells were defined as CD3+ $\gamma\delta$ TCR-CD56- and further divided into CD4+, CD8+, CD4+CD8+ and CD4-CD8- T-cells. Within total CD4+ T-cells and CD8+ T-cells, CCR7, CD45RA, CD27, and CD28 were further used to divide them into different T-cell phenotypes. B-cells were gated from the CD3- $\gamma\delta$ TCR- as CD19+ and/or CD20+ cells. B-cells were further classified as IgD+CD27-, IgD+CD27+, or IgD-CD27+/-; the IgD-CD27+/- subset was divided into plasmablasts or IgD- memory B cells based on CD20 expression and CD27. Memory cells were classified into IgM+ or IgG+. NK cells were defined within the lymphocyte gate as CD3- $\gamma\delta$ TCR- and classified as early NK (CD56+CD16-), mature NK (CD56+CD16+), and terminal NK (CD56-CD16+) cells. Dendritic cells were identified within CD3-CD19- as CD14-CD16-. Further gating identified CD123+CD45RA+ cells as plasmacytoid DCs, (pDC) and CD123-CD11c+ as classical or conventional DC (cDC). cDC were divided into type 1 (CD141+, cDC1) and type 2 (CD1c+, cDC2).

Supplementary Figure 2. Gating strategy for significant cluster validation. Statistically significant cell clusters identified in Table 1 among the different comparisons performed were further validated by identification following classical hierarchical gating approaches. C-56 was gated from central memory CD4+ CD127+ cells. C-69 was identified from early CD8 effectors as CD38+ CD314+ PD1+ CXCR3+CD95+ cells. C-37 was identified from CD8-CD4- cells as CD314+ CD45RA+ CD2+ CD159a+. C-4 subset was identified as mature NK CD45RA+ CD314+ CD14+ CCR5+ CD2+ CD57+ CD159a+ cells. C-22 was gated from non-memory CD27- cell as IgM+ CXCR3- cells. C-26 was defined as CD38+ CD141+ CD4+ CCR5+. C-27 was classified from classical monocytes as IgG+ CD38+ CD39+ CXCR3+ CD95+ cells. C-33 was gated as CD19- CD3- CD14- CD56- CXCR3+ CCR7+. C-14 was defined as CXCR3+ CD38+ basophils.

Supplementary Figure 3. Marker expression on the UMAP from peripheral blood mononuclear cells. Surface expression intensities of all 37 analysed markers are shown by a colour code based on the intensity. Red represents higher expression and blue represents lower expression

Supplementary Figure 4. Non-Responders do not recover pDC values after treatment. (A) Volcano plot of differential analysis between NR-PrePPI (n=9) and NR-PostPPI (n=9). LogFC and -Log(p-value) are represented. (B) UMAP representation from NR-PrePPI and PostPPI patients with pDC coloured. (C) Validation by classic gating of pDC as shown in Supplementary Figures 1 and 2. Boxplot with pDC represents individual percentage of total value, group median and minimum and maximum values. Red line indicates paired PrePPI and PostPPI samples. Differences were analysed by paired t-test analysis considering p-values <0.05 as statistically

949 significant (*p<0.05) (n=7). Non-Responder (NR), before treatment (PrePPI), after
950 treatment (PostPPI).

951

952 **Supplementary Table 1.** Specificity, fluorochrome, clone and provider of the different
953 antibodies used.

954

955 **Supplementary Table 2.** Cell cluster identification from control and EoE patients. For
956 each of the 73 identified FlowSOM clusters its ontogeny and subset is shown, together
957 with the specific subset, phenotype and expression of functional markers. Markers
958 highlighted in bold denote differential expression within the same population.

959

960

961

962

963

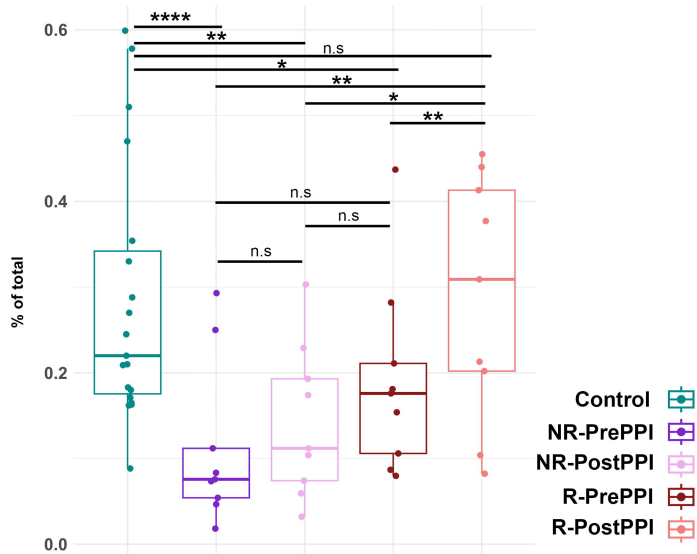
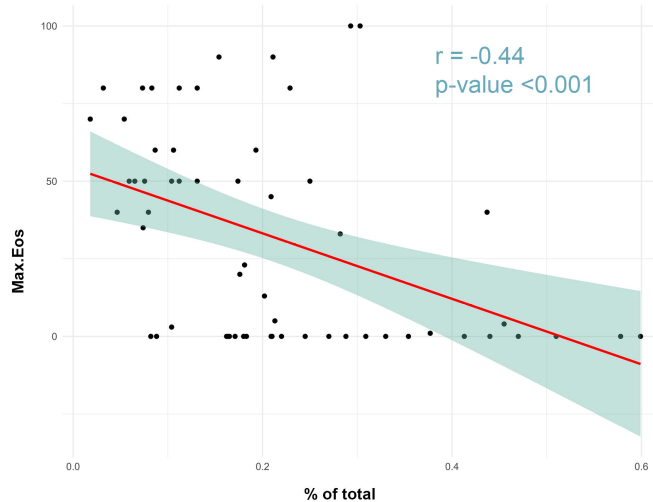
964

965

966

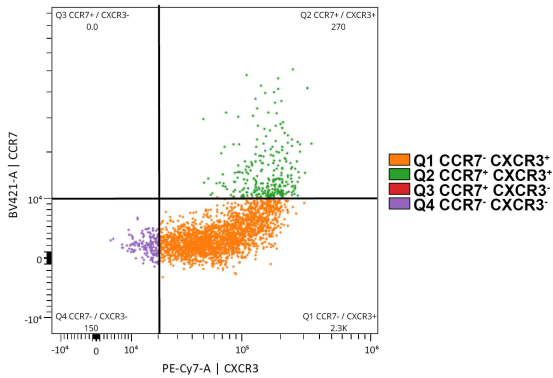
A

C-26 Dendritic cells pDC

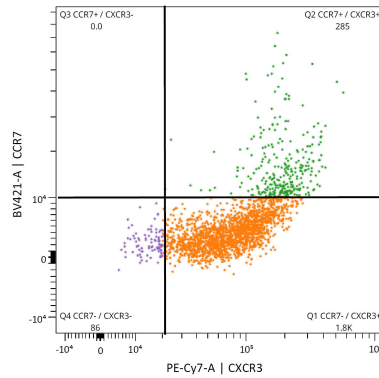
**B**

A

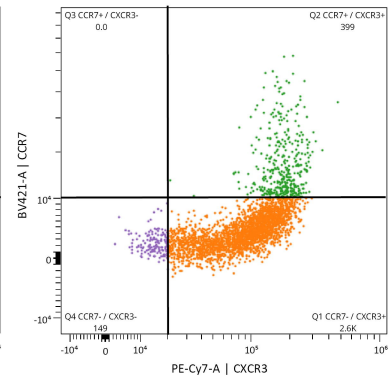
Control



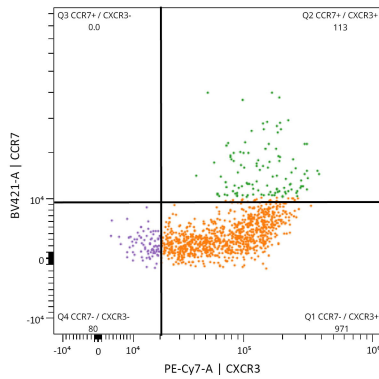
R-PrePPI



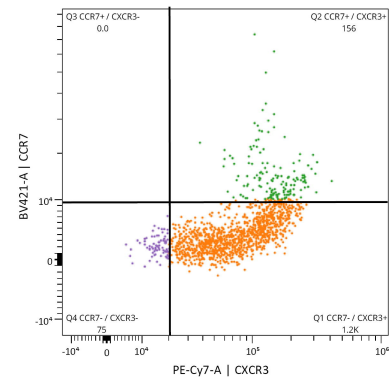
R-PostPPI



NR-PrePPI

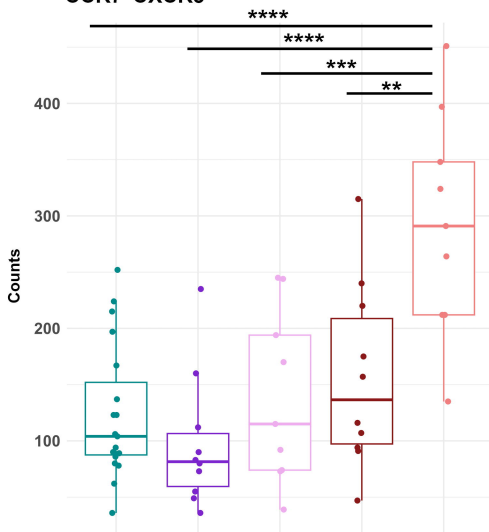


NR-PostPPI

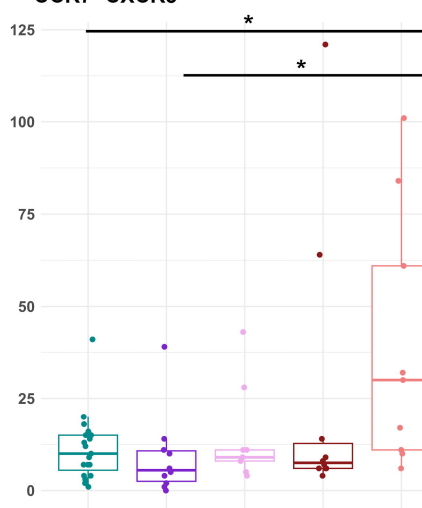


B

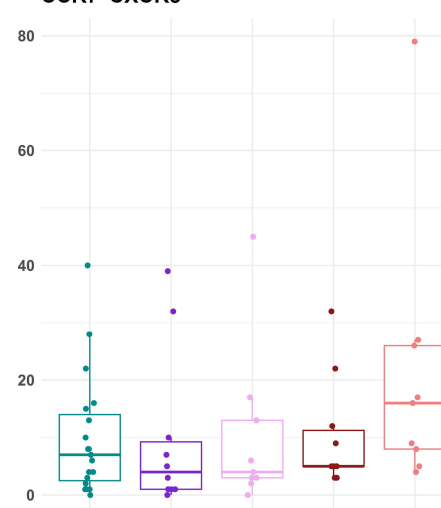
CCR7⁻ CXCR3⁺



CCR7⁺ CXCR3⁺



CCR7⁻ CXCR3⁻



Control

NR-PrePPI

NR-PostPPI

R-PrePPI

R-PostPPI

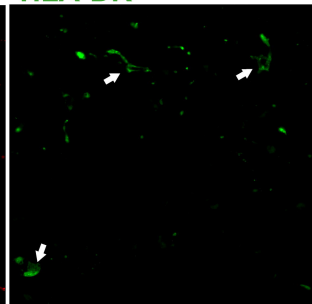
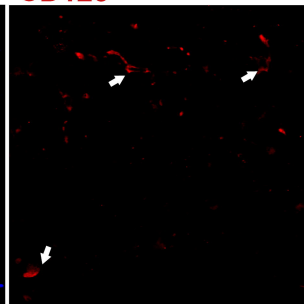
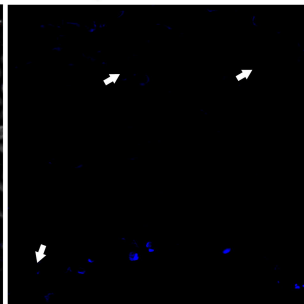
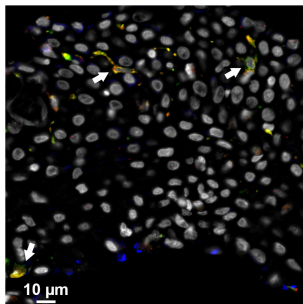
A

MERGE

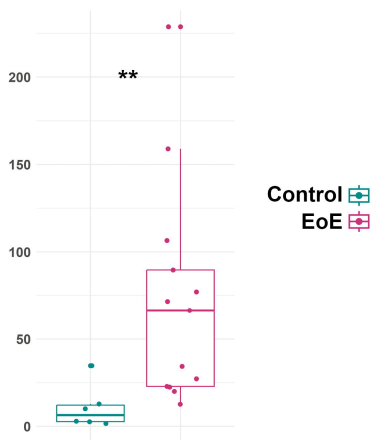
CD11c

CD123

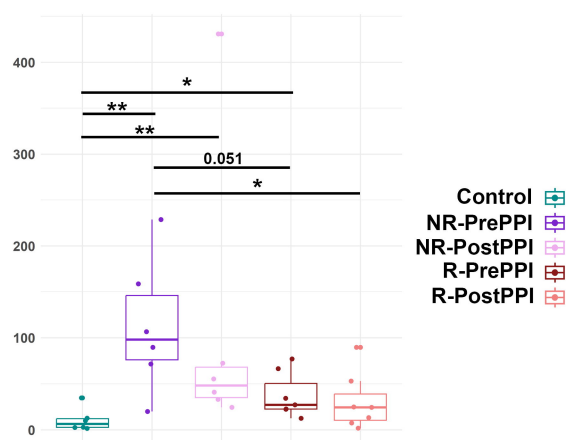
HLA-DR



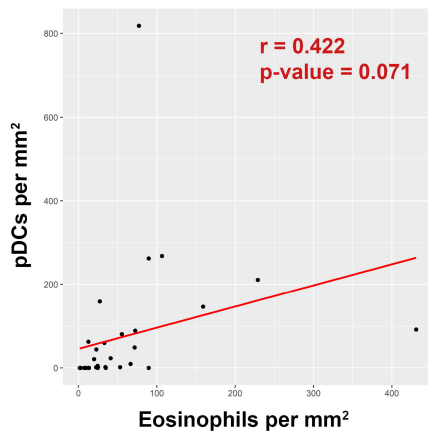
B



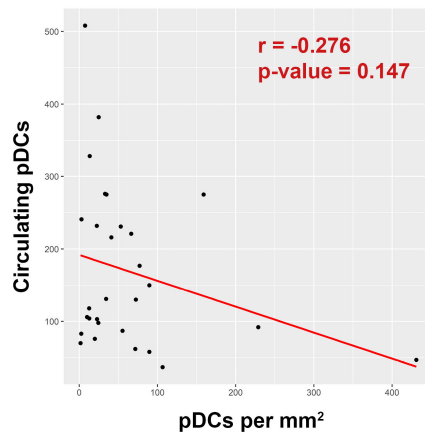
C



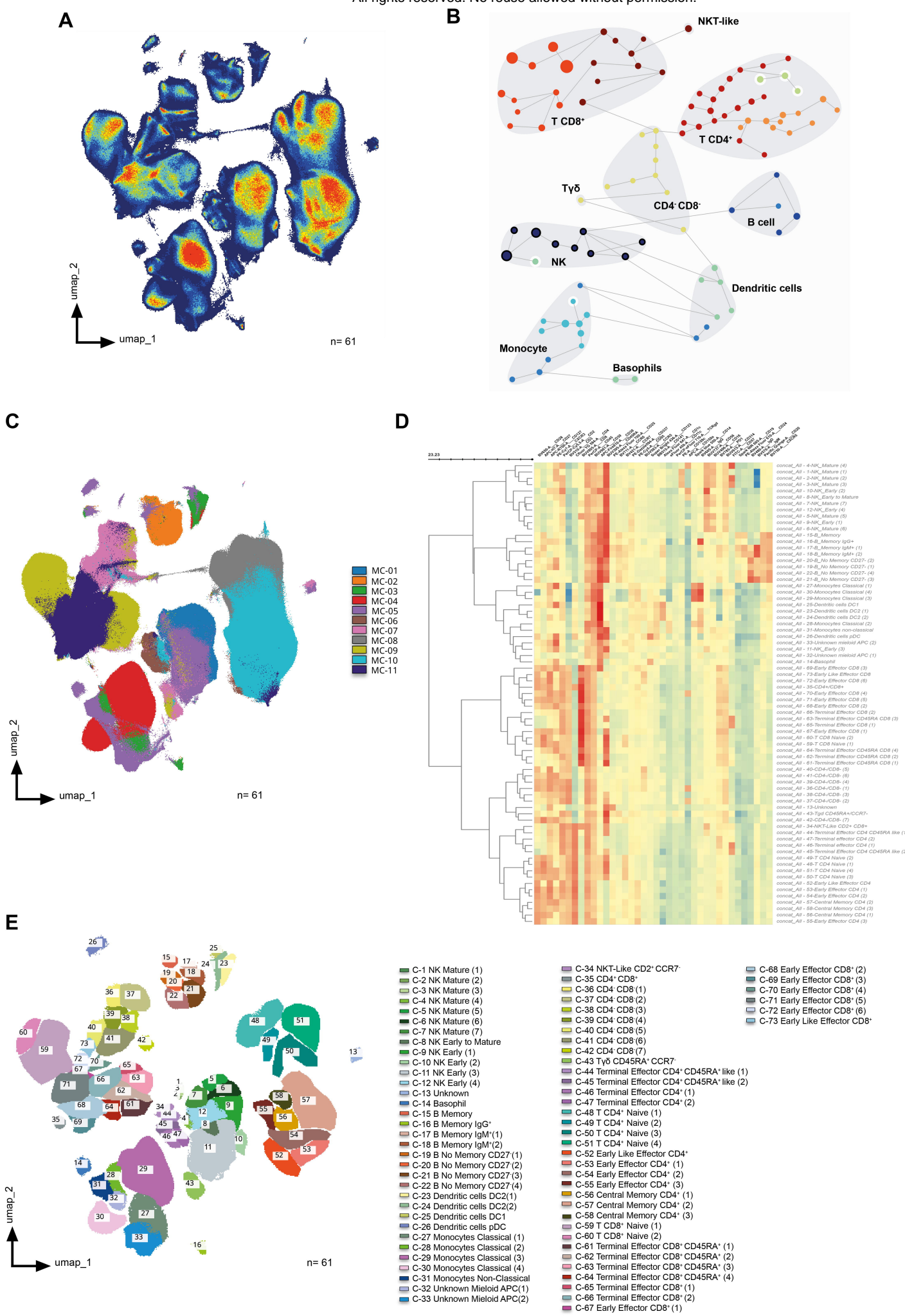
D

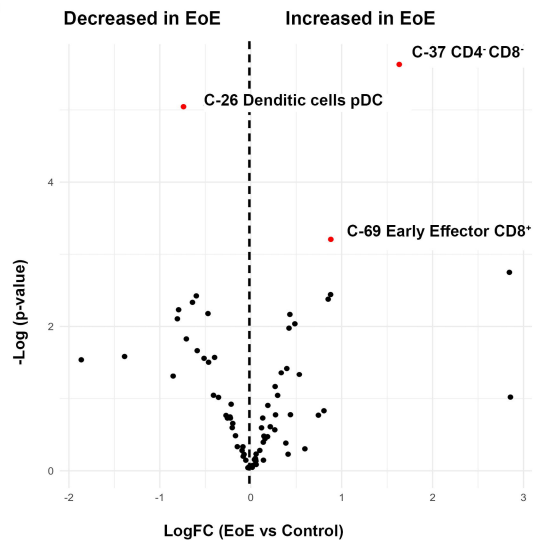
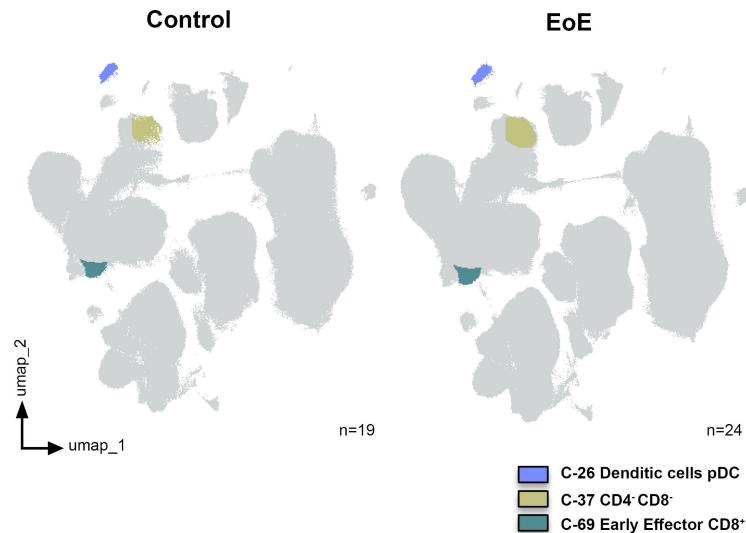
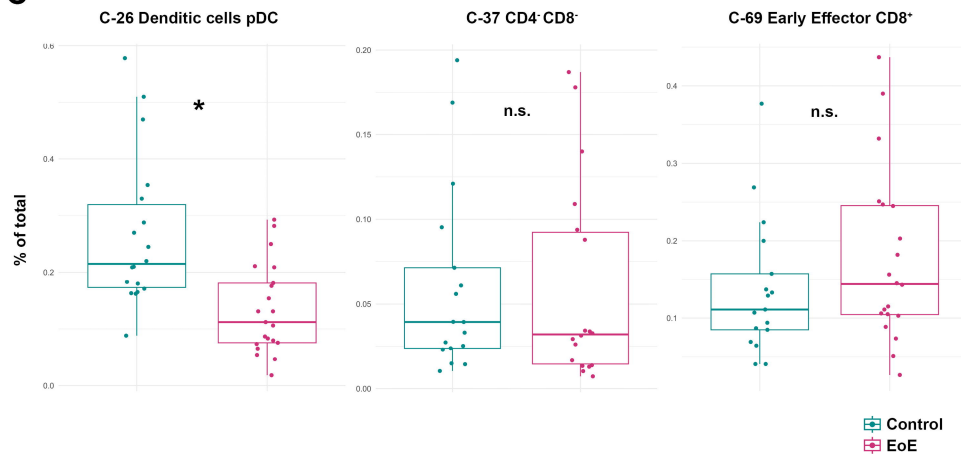


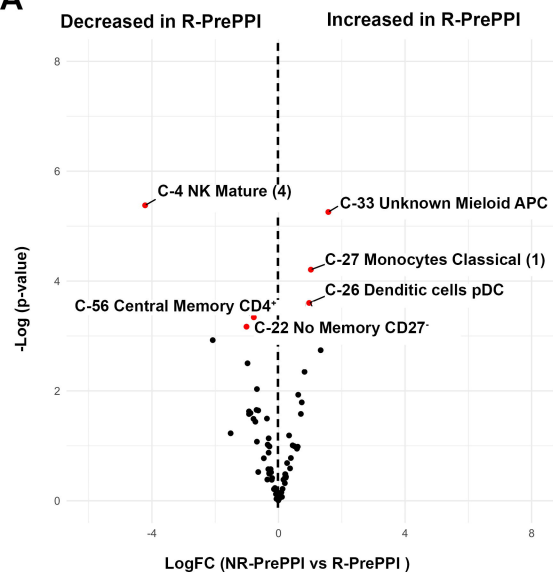
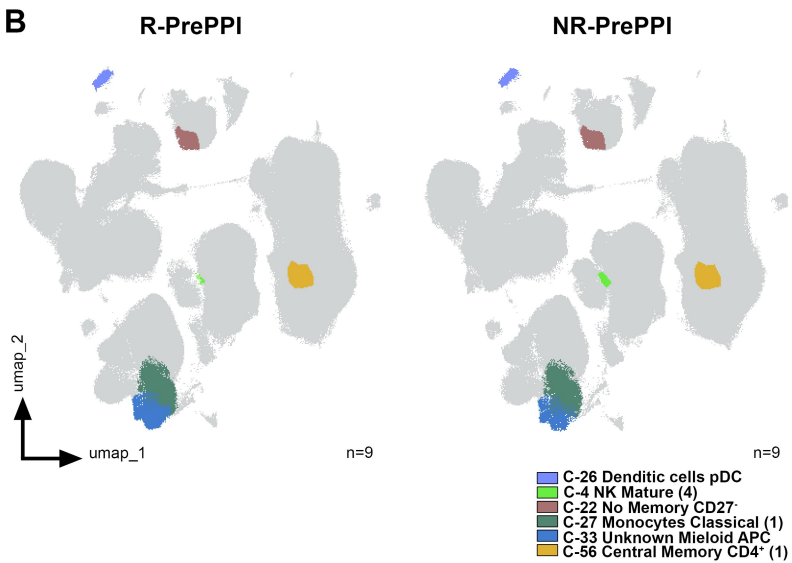
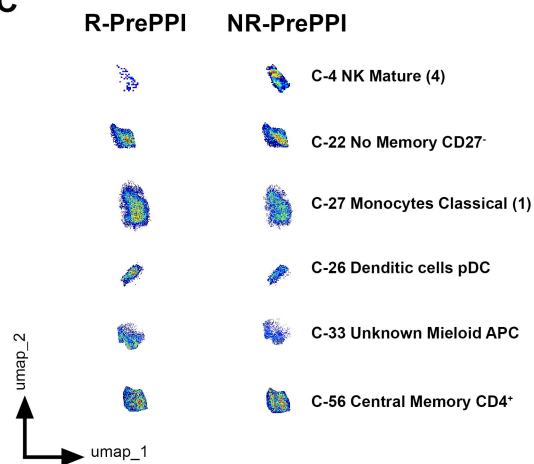
E



	Control (n=19)	EoE (n=25)	p-value	Responders (n=9)	Non-Responders (n=9)	p-value
Sex (male) (n,%)	13 (68%)	20 (80%)	0.488	7 (77%)	7 (77%)	1
Age (mean years ± s.d.)	34.42 ± 10.93	41 ± 13.7	0.060	33 ± 12.85	44 ± 14.95	0.152
<i>Symptoms (n,%)</i>						
Dysphagia	0	23 (92%)	<0.001	9 (100%)	9 (100%)	1
Food impaction	0	16 (64%)	<0.001	7 (77%)	5 (55%)	0.619
Heartburn	0	10 (40%)	0.002	3 (33%)	3 (33%)	1
Abdominal pain	0	0 (0%)	1	0 (0%)	0 (0%)	1
<i>Any atopic disease (n,%)</i>						
Asthma	0	5 (22%)	0.053	3 (33%)	1 (11%)	0.573
Allergic rhinitis/sinusitis	1 (5%)	19 (82%)	<0.001	8 (88%)	9 (100%)	1
Food allergy	2 (10%)	11 (48%)	0.0173	5 (55%)	3 (33%)	0.637
<i>Endoscopic findings (n,%)</i>						
EREFS (mean ± s.d.)	0	3.36 ± 2	<0.001	2.44 ± 2.06	3.88 ± 1.26	0.097
EREFS PostPPI (mean ± s.d.)	-	-	-	1.44± 1.51	4.33± 1	<0.001
Maximum eosinophil count (mean ± s.d.)	0	55.68 ± 23.9	<0.001	46.22 ± 21.76	65.56 ± 19.43	0.064
Maximum eosinophil count PostPPI (mean ± s.d.)	-	-	-	1.44 ± 2	65 ± 20.91	<0.001
<i>Histological findings</i>						
EoEHSS Grade (0-1) (mean ± s.d.)	0	0.50 ± 0.19	<0.001	0.43 ± 0.22	0.57 ± 0.15	0.122
EoEHSS Grade (0-1) PostPPI (mean ± s.d.)	-	-	-	0.06 ± 0.04	0.40 ± 0.22	0.006
EoEHSS Stage (0-1) (mean ± s.d.)	0	0.47 ± 0.16	<0.001	0.43 ± 0.17	0.57 ± 0.15	0.122
EoEHSS Stage (0-1) PostPPI (mean ± s.d.)	-	-	-	0.02 ± 0.03	0.31 ± 0.19	0.007
<i>PPI Treatment</i>						
Omeoprazol	-	-	-	6 (66%)	2 (22%)	0.1385
Esomeprazol				2 (22%)	2 (22%)	
Pantoprazol				1 (11%)	5 (55%)	



A**B****C**

A**B****C****D**